AD NUMBER

AD807649

LIMITATION CHANGES

TO:

Approved for public release; distribution is unlimited.

FROM:

**Distribution authorized to U.S. Gov't. agencies and their contractors;
Administrative/Operational Use; JUN 1966. Other requests shall be referred to Air Force Cambridge Research Labs., Hanscom AFB, MA.**

AUTHORITY

AFCRL ltr 22 Dec 1971

MC 65-120-R3

HIGH ALTITUDE ROCKET PLUMES

BY

PHILIP D. JARVINEN
JACQUES A. F. HILL
JAMES STARK DRAPER
R. EARL GOOD

CONTRACT NO. AF19(628)-4218
PROJECT NO. 4691 TASK NO. 469107

PERIOD COVERED: 1 JULY 1965 — 3 MAY 1966

FINAL REPORT

JUNE 1966

PREPARED FOR

AIR FORCE CAMBRIDGE RESEARCH LABORATORIES
OFFICE OF AEROSPACE RESEARCH
UNITED STATES AIR FORCE
BEDFORD, MASSACHUSETTS

MITHRAS, INC.

AEROTHERMODYNAMICS – ELECTROMAGNETICS – QUANTUM PHYSICS

701 CONCORD AVENUE, CAMBRIDGE, MASS. 02138

MITHRAS, Inc.
701 Concord Avenue
Cambridge, Massachusetts
02138

AFCRL 66-656

MC 65-120-R3

HIGH ALTITUDE ROCKET PLUMES

by

Philip O. Jarvinen
Jacques A. F. Hill
James Stark Draper
R. Earl Good

Contract No. AF19(628)-4218
Project No. 4691 Task No. 469107

Period Covered: 1 July 1965 - 3 May 1966

FINAL REPORT

JUNE 1966

Prepared for

Air Force Cambridge Research Laboratories
Office of Aerospace Research
United States Air Force
Bedford, Massachusetts

FOREWORD

This report was prepared by MITHRAS, Inc., of Cambridge, Massachusetts, for the Upper Atmosphere Physics Laboratory, Ionospheric Perturbations Branch, Air Force Cambridge Research Laboratories, L. G. Hanscom Field, Bedford, Massachusetts under Contract AF19(628)-4218.

The investigations whose results are reported here were conducted during the period 1 July 1965 to 3 May 1966. The final report was written by Mr. P. O. Jarvinen. The addendum to this report, which deals with an ionization model for high altitude rocket plumes is classified SECRET. Request for copies of the addendum should be submitted to

Mr. William F. Ring CRUR
Air Force Cambridge Research Laboratories
Laurence G. Hanscom Field
Bedford, Massachusetts

This report concludes the work on Contract AF19(628)-4218.

ABSTRACT

The gasdynamic structure of high altitude rocket plumes is investigated. A simple analytical model for the expansion of a gas into a vacuum is constructed and is shown to represent the expansion of exhaust gases from rocket motors into the region bounded by the inner shock wave and Mach disc. A comparison of the exhaust expansion model with solutions obtained with the method of characteristics is made and shows good agreement. Contours of constant density, electron density, and collision frequency in the exhaust plume of a typical rocket engine are determined. It is noted that the theory of Alden et al, which determined the geometric features of the plume surface (i.e. contact surface) may be used to define the volume in which exhaust flow properties are predicted by the exhaust expansion model. The plume scaling parameter along a typical trajectory is noted.

The blast wave theory of Hill et al is extended to allow the calculation of the size and shape of rocket plumes of solid propellant missiles. A method is derived which determines the plume drag of solid propellant motors. The method accounts for the fact that solid propellant rocket plume flow is a two phase flow of gas and solids and that the solids present in the exhaust take part in determining the mass flow but not the pressure or the expansion of the exhaust gases upon exit from the rocket nozzle. The plume expansion and resulting plume size is shown to depend on the thrust and the engine exit plane conditions of the gas phase of the two phase flow.

A method is described which allows the average properties in the air-exhaust gas layer on the periphery of the plume to be evaluated. The variation of mass flow, velocity, pressure, temperature and overall thickness along the layer is ascertained. The analysis is extended to give the average properties of the air layer between the dividing streamline and the outer shock and the exhaust gas layer on the inside.

The theory of Whitham (1952) which describes the far-field flow about supersonic axisymmetric bodies, is used to evaluate the plume drag and is found to be in agreement with the blast wave predictions of Hill et al.

In the addendum to this report, a high altitude plume ionization model is developed using the theoretical models for exhaust flow, two phase rocket motor flow and properties of the air-exhaust gas layer.

TABLE OF CONTENTS

LIST OF FIGURES

1. INTRODUCTION

The aerodynamic features in the nose region of a high altitude plume are shown in Figure 1. The rocket motor exit plane pressure is many orders of magnitude larger than the local ambient pressure. The exhaust gases expand rapidly after exit from the rocket motor, reaching a maximum angle of expansion θ_M which is determined by the rocket motor exit Mach number and the ratio of specific heats, γ, of the exhaust gases. The exhaust gas plume appears as a blunt body to the free stream flow and a bow shock wave is formed about the plume. The free stream flow which passes through the bow shock, flows outward in the region between the bow shock and the contact surface. The internal shock wave is formed in a not too obvious way by the coalescence of compression waves from the jet edge. These waves are simply reflections of expansion waves formed at the exit of the underexpanded nozzle. The expanding exhaust gases are deflected into the downstream direction by the free stream flow and are confined to the region to the right of the contact surface. The exhaust gases which pass through the inner shock flow outward in the region between the contact surface and the inner shock wave (i.e., streamtube AB). Exhaust gases expand into the region bounded by the inner shock wave and Mach disc as if into a vacuum. The launch vehicle is immersed in a layer between the bow and inner shocks and plays a negligible part in determining the flow characteristics. The flow is hypersonic and continuum theory holds.

Analytical techniques have previously been developed which describe the inviscid gasdynamic structure of high rocket plumes. Hill et al (1963) developed a simple theory to describe the size and shape of the plumes of expanding gases behind a missile in powered flight at altitudes above 100 km using the blast-wave analogy. Expressions were derived for the rocket plume nose radius, maximum plume diameter and distance to the Mach disc. A comparison of the theoretical predictions with optical observations of Atlas and Titan plumes showed excellent agreement in the nose radii and maximum radii of the plumes.

This theory relates the plume parameters, such as nose radius, to the plume drag. The relationship between plume drag and engine thrust is determined by applying a momentum balance to the rocket plume. It is shown that the geometric features of the plume can be described if the engine thrust and thrust coefficient, vehicle altitude and forward speed are known.

Alden et al, (1964) developed a simple inviscid analytical theory which defined the geometrical features of the plume surface (i.e., contact surface) by applying a force-momentum balance to the plume and determined a one-parameter family of functions which described the jet flow from rocket motors. In addition, the validity of using continuum fluid mechanics to describe high altitude plume phenomenon was examined.

In this report some additional theoretical models for the inviscid gasdynamic structure of high altitude plumes are discussed. An improved analytic method for calculating the expansion of gas from the exit of a rocket nozzle into the region bounded by the inner shock wave and Mach disc is constructed. The method is especially useful for high altitude calculations where the plume extends for thousands of nozzle exit radii and where the method of characteristics, while capable in principle of describing the exhaust gas flow, has practical limitations such as its relatively high cost and the difficulty of calculating more than a few hundred radii from the nozzle exit. A comparison of the exhaust expansion model with solutions obtained with the method of characteristics is made and shows good agreement. Contours of constant density, electron density and collision frequency in the exhaust plume of a typical rocket engine are determined using this exhaust model.

The blast wave theory of Hill, et al, is extended to allow the calculation of the size and shape of rocket plumes of solid propellant missiles. A method is derived which determines the plume drag of solid propellant motors. The method accounts for the fact that solid propellant rocket plume flow is a two phase flow of gas and solids and that the solids present in the exhaust take part in determining the mass

flow but not the pressure or the expansion of the exhaust gases upon exit from the rocket nozzle. The plume expansion and resulting plume size is shown to depend on the thrust and the engine exit plane conditions of the gas phase of the two phase flow.

A method is described which allows the average properties in the air-exhaust gas layer on the periphery of the plume to be evaluated. The variation of mass flow, velocity, pressure, temperature and overall thickness along the layer is ascertained. The analysis is extended to give the average properties of the air layer between the dividing streamline and the outer shock and the exhaust layer on the inside.

2. ANALYTIC DESCRIPTION OF PLUME FLOWS

The expansion of a gas from the exit of a rocket nozzle into a vacuum may be calculated in a straightforward manner by the numerical method of characteristics. Although most of the published calculations consider the thermodynamic behavior of the gas to be perfect, this restriction is not necessary.

In most rocket plume problems of interest the expansion is into a finite back pressure rather than into a vacuum. A shock wave then forms in the jet near its outer boundary. The vacuum solution is useful, however, in that it still describes the flow inside the region bounded by this shock. It may also be used to calculate the shock envelope in the manner described by Alden et al.

Now the method of characteristics, while capable in principle of describing the flow from any rocket motor, has two practical limitations. One is its relatively high cost and the other the difficulty of carrying out the calculations more than a few hundred radii from the nozzle exit. Thus a simple analytic method may be very useful, especially for high-altitude calculations where the plume extends for thousands of nozzle exit radii. Such a method, drawing on information available from exact solutions, is given below.

2.1 General Character of Plume Flows

A schematic illustration of the flow exhausting from a nozzle into a vacuum is given in Figure 2. The expansion is bounded by the limiting streamline at the angle θ_{max}, which represents a Prandtl-Meyer flow at the nozzle lip. Along the other stream-lines the flow turns more gradually but "exact" calculations show that as the local velocity approaches the maximum possible velocity, V_m, all streamlines become essentially straight. This behavior is in fact characteristic of any irrotational flow pattern in which the velocity variation from one streamline to the next tends to zero.

With the velocity fixed in the far field of the flow pattern, conservation of mass along any streamtube requires an inverse square law variation of density with radial distance from the exit. It is known, moreover, that the mass flux is a maximum along the axis and falls off very rapidly with angle of inclination from the axis. A complete simple description of the flow can be given by specifying this angular distribution of mass flux.

2.2 Angular Distribution of the Mass Efflux

2.2.1 One Parameter Family of Distribution

In our approximate description of the flow far from the nozzle the streamlines are straight and appear to originate from a common point close to the center of the nozzle exit. Along each streamline we have

$$\rho V r^2 = \text{constant} = d\dot{m}^{o}(\theta) \tag{1}$$

where

ρ is the density

V is the velocity

r is the radial coordinate

The quantity $d\dot{m}^{o}(\theta)$ represents the mass flux per unit solid angle in the direction θ.

It is convenient to normalize $d\dot{m}^{o}(\theta)$ with respect to its value on the nozzle axis and to write

$$f(\theta) = \frac{d\dot{m}^{o}(\theta)}{d\dot{m}^{o}(0)} = \frac{(\rho V r^2)_\theta}{(\rho V r^2)_0} \tag{2}$$

We then postulate that a one-parameter family of functions $f(\theta)$ is sufficient to describe adequately the flow from all nozzles.

A suitable form of the function $f(\theta)$ may be obtained from some available "exact" solutions by the method of characteristics. Alden et al (1964) has suggested the form

$$f(\theta) = \left[\frac{\cos\theta - \cos\theta_{max}}{1 - \cos\theta_{max}}\right]^m$$

where θ_{max} is the limiting flow inclination for expansion into a vacuum. A somewhat better fit to a larger sample of exact calculations has since been obtained with the function

$$f(\theta) = \exp\left[-\lambda^2(1 - \cos\theta)^2\right] \qquad (3)$$

A typical sample of "exact" results plotted in a coordinate system appropriate to this function is shown in Figure 3. Because data on the axis was not available in these cases we have plotted the function

$$\frac{(\rho V r^2)_0}{\rho^* a^* r^{*2}} \quad f(\theta) = F(\theta) \qquad (4)$$

The value of the constant multiplier of $f(\theta)$ varies from one nozzle to the next.

Unlike Alden's (1964) function, this new one does not satisfy the condition

$$f(\theta_{max}) = 0$$

However, as shown in Figure 3, $f(\theta_{max})$ is certainly extremely small and the contribution of the fictitious mass flux beyond θ_{max} to calculations of total mass and momentum fluxes is safely neglected.

2.2.2 Determination of the Value of the Parameter λ

The parameter λ is determined by requiring that the mass and momentum fluxes in the flow equal those at the nozzle exit. These fluxes may be computed by integrating over the solid angle containing the flow. We shall regard this integration as being performed over a surface and in particular we shall use constant-property surfaces on which the values of the density, velocity, etc., are constant.

The total mass flux in the flow may be written

$$\dot{m} = 2\pi \int_0^{\theta_{max}} \rho V r^2 \sin\theta \, d\theta$$

$$= 2\pi (\rho V r^2)_0 \int_0^{\theta_{max}} f(\theta) \sin\theta \, d\theta$$

$$= \pi \rho^* a^* r^{*2} \qquad (5)$$

where the superscript * refers to conditions at the nozzle throat.

The momentum balance between the constant-property surface and the nozzle exit plane may be written

$$F = 2\pi (\rho V r^2)_0 V \int_0^{\theta_{max}} f(\theta) \cos\theta \sin\theta \, d\theta + p A_{ex}$$

$$= \pi C_F p_c r^{*2} \qquad (6)$$

where

F is vacuum thrust of the nozzle

A_{ex} is the nozzle exit area

V is the velocity on the integration surface

p is the pressure on the integration surface

p_c is the combustion chamber pressure

C_F is the vacuum thrust coefficient

Now in the far field p/p_c is very small and the contribution of the pressure term may be neglected. Dividing the first expression into the second we obtain

$$\frac{\int_0^{\theta_{max}} f(\theta) \cos\theta \sin\theta \, d\theta}{\int_0^{\theta_{max}} f(\theta) \sin\theta \, d\theta} = \frac{C_F p_c}{\rho^* a^* V} \tag{7}$$

Now it may be shown that:

$$\frac{\rho^* a^* V_m}{p_c} = C_{F_{max}} \tag{8}$$

where

V_m is the limiting velocity

$C_{F_{max}}$ is the maximum vacuum thrust coefficient

Thus

$$\frac{C_F p_c}{\rho^* a^* V} = \frac{C_F V_m}{C_{F_{max}} V} = \frac{C_F}{w C_{F_{max}}} \tag{9}$$

The integrals are conveniently evaluated in terms of the parameter λ by making the substitution

$$\eta = 1 - \cos\theta \tag{10}$$

and, in view of the small value of the integrand at θ_{max}, letting the upper limit of $\eta \to \infty$. Thus

$$\frac{C_F}{w\, C_{F_{max}}} = \frac{\int_0^\infty e^{-\lambda^2 \eta^2} (1 - \eta)\, d\eta}{\int_0^\infty e^{-\lambda^2 \eta^2}\, d\eta} = 1 \pm \frac{1}{\lambda\sqrt{\pi}} \tag{11}$$

Choosing the sign to yield a positive value for λ we finally obtain

$$\lambda = \frac{1}{\sqrt{\pi}} \frac{1}{1 - C_F/w\, C_{F_{max}}} \tag{12}$$

2.3 Properties of Typical Flows

2.3.1 Variation of λ

The value of the parameter λ as derived above depends on

(a) the quantity $C_F/C_{F_{max}}$ which is fixed by the characteristics of the propellant and rocket nozzle

(b) the velocity ratio w which varies from one constant-property contour to the next

For the asymptotic flow at very large distances from the exit $w \to 1$ and the constant-property contours become self-similar, fixed by the parameter $C_F/C_{F_{max}}$. Figure 4 illustrates the variation of λ_∞, the asymptotic value of λ, with the nozzle area ratio and the value of γ (ratio of specific heats) of the exhaust gases. For any given rocket motor the value of λ varies along the plume. This is illustrated in Figure 5 for a set of nozzles with $A/A^* = 25$.

2.3.2 Density Decay Along the Axis

The mass-flux balance (5) above may be manipulated to yield

$$\frac{(\rho r^2)_0}{\rho^* r^{*2}} = \frac{\lambda}{\sqrt{\pi}} \frac{w^*}{w} \tag{13}$$

for the variation of density along the axis. Normalizing the density with respect to its value in the combustion chamber,

$$\frac{(\rho r^2)_0}{\rho_c r^{*2}} = \left[\frac{2}{\gamma + 1}\right]^{\frac{1}{\gamma - 1}} \frac{\lambda}{\sqrt{\pi}} \frac{w^*}{w} \tag{14}$$

For a given value of ρ/ρ_c, then the axial station, $(r)_0 = x$, is given by

$$\left(\frac{x}{r^*}\right)^2 = \left[\frac{2}{\gamma + 1}\right]^{\frac{1}{\gamma - 1}} \frac{\lambda}{\sqrt{\pi}} \frac{w^*}{w} \frac{\rho_c}{\rho} \tag{15}$$

Thus the rate of density decay depends primarily on the value of λ, but is modified near the nozzle by the variation in w. In the asymptotic flow with $w \approx 1$.

$$\frac{\rho}{\rho_c} \left(\frac{x}{r^*}\right)^2 = \left[\frac{2}{\gamma + 1}\right]^{\frac{1}{\gamma - 1}} \frac{\lambda_\infty}{\sqrt{\pi}} w^* \tag{16}$$

with a constant of proportionality dependent on λ_∞ and γ. Figure 6 shows the variation of density along the axis for three values of γ. The value of λ_∞ in each case has been chosen to correspond to an area ratio $A/A^* = 25$. Note that the higher densities persist further with the higher values of γ.

2.3.3 Constant Density Contours

Once we have located the point on the axis corresponding to any given density the rest of the curve along which the density has this value is given by the equation

$$\frac{r^2(\theta)}{r^2(0)} = f(\theta) = \exp\left[-\lambda^2 (1 - \cos\theta)^2\right] \tag{17}$$

that

$$x = r_0 \cos\theta \exp\left[-\lambda^2 (1 - \cos\theta)^2/2\right] \tag{18}$$

$$y = r_0 \sin\theta \exp\left[-\lambda^2 (1 - \cos\theta)^2/2\right] \tag{19}$$

Figure 7 illustrates typical constant property contours for the three values of γ used in Figure 6. As expected, the narrower plumes are those in which high densities persist further downstream.

2.4 Comparison with Published Numerical Solutions

2.4.1 Density Decay Along the Axis

In a discussion of a different far-field approximation for plume flows, Sibulkin and Gallaher (1963) have published the results of some numerical calculations by the method of characteristics. They describe the rate of density decay along the axis of the flow in terms of the parameter

$$B = \frac{\rho}{\rho_c} \left(\frac{x}{d^*}\right)^2 \tag{20}$$

evaluated at $x/r_e = 100$ for $\gamma = 1.2$, 1.3 and 1.4 and at $x/r_e = 50$ for $\gamma = 1.67$.

In terms of the theory of this report,

$$B = \left[\frac{2}{\gamma + 1}\right]^{\frac{1}{\gamma - 1}} \frac{\lambda}{4\sqrt{\pi}} \frac{w^*}{w} \qquad (21)$$

In Figure 8, this formula is compared with the computations quoted by Sibulkin and Gallaher (1963). The agreement is good. The approximate theory errs on the low side for the lower values of γ but by not more than 30 percent at most. This error is much smaller than that of Sibulkin and Gallaher's (1963) method.

2.4.2 Constant-Property Contours

A typical set of constant-property contours calculated numerically by the method of characteristics has been published by Altshuler (1958). This set is restricted to the region near the nozzle exit where the flow has not yet become asymptotic so that the value of λ changes appreciably from one contour to the next.

Figure 9 illustrates the three contours furthest from the nozzle together with the predictions of the approximate method of this report. The agreement is good and improves with increasing distance as expected. At the larger distances for which this analytic method is intended it should yield a flow pattern accurate enough for any engineering application.

2.5 Contours of Constant Electron Density and Collision Frequency In a Typical Plume.

The exhaust flow expands as if into a vacuum upon exit from rocket motors operating at high altitudes. The rapid expansion causes the flow downstream of the exit plane to be frozen (i.e., no chemical reactions occur to change the exhaust gas composition or electron

population). Downstream of the engine exit plane the electron density varies exactly as the gas density. Thus contours of constant gas density are also contours of constant electron density (plasma frequency). The same contours also represent constant collision frequency contours. A knowledge of the gas density, electron density and collision frequency at the nozzle exit plane in conjunction with the engine γ is sufficient to define these parameters throughout the exhaust flow within the inner shock and Mach disc. Electron density and collision frequency contours have been evaluated for a typical engine using the analytical model for exhaust flow into a vacuum and assuming frozen flow downstream of the nozzle exit plane. (Figure 10). The initial electron density and collision frequency at the engine exit plane were normalized to 1.0 electron per cubic centimeter and 1.0 collision per second respectively.

2.6 Locations of Plume Surface

Alden et al, developed a simple, analytic, inviscid theory to describe the surface of rocket plumes. The surface of the plume is described by the dividing streamline (contact surface) separating the outer air flow from the inner flow of rocket exhaust gases. The location of the surface is determined by formulating a force-momentum balance normal to the plume surface in conjunction with a model for the exhaust flow field and the assumption that hypersonic flow theory is applicable. The inviscid plume surface is found to be represented by a nondimensional, second order non-linear differential equation in terms of $\bar{r}$ and θ (Figure 11), the nondimensional spherical radius and polar angle respectively, which when integrated located the surface of the dividing streamline. The differential equation contains, in addition to the coordinate variables ($\bar{r}$, θ), only two explicit parameters (γ, θ_M), which are fixed by the rocket motor exhaust properties and geometry. The effects of all other parameters (i.e., combustion pressure, motor size, forward

speed and altitude) are combined implicity in $\bar{r}$ which is defined as

$$\bar{r} = \left(\frac{q_o}{P_c}\right)^{1/2} \frac{r}{y^*} \qquad (22)$$

q_o = free stream dynamic pressure

P_c = engine chamber pressure

y^* = engine throat radius

For a given motor type, a single computation will give the plume shape for all (high) altitudes, all motor sizes, various chamber pressures, and all hypersonic flight speeds. A typical plume contact surface shape, calculated using this method, is shown in Figure 12 for $\gamma_{jet} = 1.25$ and maximum Prandtl-Meyer expansion angles θ_M of 120.5°, corresponding to exit Mach number of 3.

Dimensional contact surface geometries (r as a function of θ) may be obtained from the non-dimensional results through the scaling factor

$$\left(\frac{q_o}{P_c}\right)^{1/2} \frac{1}{y^*} .$$

The variation of the plume scaling parameter along a representative trajectory is noted in Figure 13. The size of the plume is seen to change by one order of magnitude between 90 and 120 kilometers and approximately another order of magnitude between 120 and 180 kilometers. The exhaust flow within the inner shock wave (approximately represented by the contact surface) remains unmodified by external flow conditions. Therefore superposition of the dimensional contact surface geometry on dimensional electron density contours specifies the volume in which exhaust flow properties as predicted by the exhaust expansion model are unmodified by the external flow field.

As noted in the following section, the plume surface for solid propellant rocket motors is properly located with the theory of Alden et al if the gas phase exhaust properties of the two phase flow are used.

3. PLUMES GENERATED BY SOLID PROPELLANT MOTORS

3.1 General Theory of Plume Drag

The rocket nozzle flow from solid propellant motors is a two-phase flow of gas and solids and parameters such as C_p, R, C_v and γ must be determined differently than for single phase gas flow.

Simple calculations of two-phase nozzle flows can be made once the effective mean C_p, R and γ for the gas phase, the effective mean C_p for the solid phase and the relative weight flows of the gas and solid phases are determined.

For a mixture of gases, the mole fraction n_{i_o} is defined as the ratio of the number of moles present of the i^{th} component to the total number of moles, both per unit volume. Thus

$$n_{i_o} = \frac{n_i}{\Sigma n_i} = \frac{n_i}{n} \tag{23}$$

The mass concentration is

$$C_i = \frac{M_i \; n_{i_o}}{\Sigma_i M_i n_{i_o}} \tag{24}$$

where M_i is the molecular weight of the i^{th} component. The specific heat C_p, for a mixture is the sum of the component specific heats weighted according to their respective mass fractions C_i, as follows:

$$C_p = \Sigma_i \; C_i \; C_{p_i} \tag{25}$$

The gas constant for the mixture is determined from the universal gas constant $\hat{R}$ and the molecular weight of the mixture M

$$R = \hat{R}/M \tag{26}$$

The ratio of specific heats, γ, for the mixture of gases is obtained from C_p and R as follows

$$C_v = C_p - R \tag{27}$$

$$\gamma = C_p/C_v \tag{28}$$

The effective values of $\overline{\gamma}$, $\overline{R}$ and $\overline{C}_p$ for the gas-solid rocket motor flow are formed from the following expressions,

$$\overline{\gamma} = \gamma \frac{1 + K C_{p_s}/C_p}{1 + \gamma K C_{p_s}/C_p} \tag{29}$$

$$\overline{R} = \frac{R}{1 + K} \tag{30}$$

$$\overline{C}_p = \frac{C_p + K C_{p_s}}{1 + K} \tag{31}$$

where

$$K = \frac{\text{mass flow of solids}}{\text{mass flow of gas}} \tag{32}$$

C_{p_s} = effective specific heat of solids (33)

The nozzle flow conditions for the study engine are obtained from gas flow tables (Wang et al (1957)) using the engine expansion ratio, A_e/A^*, and the effective specific heat ratio γ.

The following ratios are obtained;

$$V_e/V_M = C_1 \tag{34}$$

$$M_e = C_2 \tag{35}$$

$$P_e/P_c = C_3 \tag{36}$$

$$T_e/T_c = C_4 \tag{37}$$

The maximum gas velocity, V_M, is determined from (34)

$$V_M = V_e/C_1 \tag{38}$$

where V_e, the exit velocity, is usually a specified engine characteristic or is calculated for a properly expanded engine as

$$V_e = g\, I_{SP}$$

The chamber temperature, T_c, is

$$T_c = \frac{V_M^2}{2\,\bar{C}_p} \tag{39}$$

The exit temperature (37) is

$$T_e = T_c\, C_4 \tag{40}$$

The exit pressure (36) is

$$P_e = P_c\, C_3 \tag{41}$$

where P_c, the chamber pressure, is usually a specified engine characteristic.

The engine thrust coefficient as evaluated from the previously derived parameters is (Hill et al (1963))

$$C_F = \sqrt{\frac{2\bar{\gamma}^2}{\bar{\gamma}-1}\left(\frac{2}{\bar{\gamma}+1}\right)^{\frac{\bar{\gamma}+1}{\bar{\gamma}-1}}\left[1-\left(\frac{P_e}{P_c}\right)^{\frac{\bar{\gamma}-1}{\bar{\gamma}}}\right]} + \left(\frac{A_e}{A^*}\right)\left(\frac{P_e}{P_c}\right) \quad (42)$$

and the maximum thrust coefficient is

$$C_{F_{max}} = \frac{2\bar{\gamma}}{\sqrt{\bar{\gamma}^2-1}}\left(\frac{2}{\bar{\gamma}+1}\right)^{1/\bar{\gamma}-1} \quad (43)$$

At this point, a check may be made on the calculations by comparing the thrust coefficient as calculated from expression (42) with that derived from specified engine characteristics

$$\bar{C}_F = \frac{T}{P_c A^*} \quad (44)$$

or by comparing the total engine thrust calculated from

$$T = \bar{C}_F P_c A^* \quad (45)$$

with the specified engine thrust. The throat area A* and expansion ratio A_e/A^* are usually specified quantities.

The plume drag of a rocket with two phase (gas and solid) flow should be calculated using the thrust due to gas alone since the solid particles do not take part in the expansion. The speed of sound in the gas along governs the expansion of the plume at large pressure ratios. The frozen (gas along) Mach number is

$$M_g = \frac{V_e}{\sqrt{\gamma R T_e}} \quad (46)$$

The Mach number is considerably lower than the equilibrium (including solids) Mach number. The thrust of the rocket engine due to the gas phase is calculated by determining the chamber conditions

corresponding to the gas along exit conditions, γ and M_g. From gas tables, the following pseudo engine characteristics are obtained

$$\left(\frac{A_e}{A^*}\right)_P \tag{47}$$

$$\left(\frac{P_e}{P_c}\right)_P \tag{48}$$

The chamber pressure and throat area of the pseudo engine are determined since the exit pressure and exit area are known quantities.

The pseudo engine thrust coefficient is

$$C_{F_P} = \sqrt{\frac{2\gamma^2}{\gamma-1}\left(\frac{2}{\gamma+1}\right)^{\frac{\gamma+1}{\gamma-1}}\left[1-\left(\frac{P_e}{P_c}\right)_P^{\frac{\gamma-1}{\gamma}}\right]} + \left(\frac{A_e}{A^*}\right)_P\left(\frac{P_e}{P_c}\right)_P \tag{49}$$

The maximum thrust coefficient is

$$C_{F_{max\ P}} = \sqrt{\frac{2\gamma}{\gamma^2-1}}\left(\frac{2}{\gamma+1}\right)^{1/\gamma-1} \tag{50}$$

The rocket thrust (gas alone) is

$$T_g = \left(C_F\right)_P\left(P_c\right)_P\left(A^*\right)_P \tag{51}$$

For comparison, the gas thrust can also be determined from

$$T_g = T\,(1-\lambda) \tag{52}$$

where

$$\lambda = \frac{\text{mass flow of solids}}{\text{total mass flow}} \tag{53}$$

For a solid fueled rocket, the plume drag is

$$D = T_g \left[\frac{\left(C_{F_{max}}\right)_P}{\left(C_F\right)_P} - 1 \right] \qquad (54)$$

The plume drag for a specific engine may be determined once the physical characteristics of the motor, exhaust product composition and exhaust component specific heats are specified. Since the mass flow of solids may represent up to 40 percent by weight of the overall two phase flow, the thrust due to the gas phase may be as low as 60 percent of the overall engine thrust. For a typical engine, the plume drag may equal from fifteen to twenty-five percent of the overall thrust. The plume drag is the amount of thrust lost through improper expansion of the exhaust gases (i.e., engine exit pressure does not equal ambient pressure). For the instances where the thrust of the rocket engine varies with time, the magnitude of the plume drag will also vary with time. Multiple nozzle configurations may be treated by defining an equivalent single nozzle configuration.

3.2 Plume Characteristics

With the plume drag determined, the blast wave theory of Hill 1963 et al may be used to calculate the geometric features of the exhaust plume such as the plume nose radius of curvature, maximum diameter and distance to the Mach disc.

The plume nose radius of curvature is

$$R = .40 \sqrt{\frac{\gamma_\infty}{J_o}} \sqrt{\frac{D}{\rho_\infty V_\infty^2}}$$

γ_∞ free stream ratio of specific heats

J_o a constant equal to .85

D the plume drag

ρ_∞ free stream density

V_∞ vehicle velocity

The maximum plume radius is

$$r_{max} = \sqrt{\frac{2}{\pi}} \sqrt{\frac{1}{C_D}} \sqrt{\frac{D}{P_\infty M_\infty^2}}$$

C_D Drag coefficient of plume shape

P_∞ free stream pressure

M_∞ free stream Mach number

The distance to the Mach disc is

$$L = \frac{1}{2} \sqrt{\frac{\gamma^2 - 1}{\pi}} \frac{V_\ell}{V_{e_x}} \frac{M_{e_x}}{\sqrt{1 + \frac{1}{\gamma M_{e_x}^2}}} \sqrt{\frac{T_g}{P_\infty}}$$

V_ℓ limiting velocity of exhaust gas flow

V_{e_x} exhaust gas velocity at exit planes

M_{e_x} exit plane Mach number

T_g thrust due to gas phase flow

γ ratio of specific heats for gas phase flow

4. AVERAGE PROPERTIES IN THE AIR-EXHAUST LAYER

With the contact surface positioned, it is possible to derive simplified properties of the double shock layer (air-exhaust gas layer on the periphery of the plume) using the inviscid model outlined by Alden et al. By treating the layer as if it were a mixture of two gases, instead of being separated by a contact surface, it is possible to estimate the overall thickness of the layer and its average properties. The thickness of the layer may be expressed in non-dimensional form and is a function only of position along the dividing streamline (i.e., contact surface), the properties of the exhaust gases and the ratio of the free stream velocity to the jet limiting velocity. In functional form, $\overline{\delta}_{ML}$ is

$$\overline{\delta}_{ML} = F\left\{ \overline{r},\ \theta,\ \gamma_j,\ \theta_M,\ V_\infty/V_M \right\} \tag{55}$$

A new parameter, V_∞/V_M, appears in the determination of the overall thickness of the air-exhaust gas layer. It is interesting to note that this parameter influences the thickness of the double shock layer but does not influence its position.

4.1 Properties of Air and Exhaust Gas Layer

The analysis may be extended to provide the properties of the individual layers. (i.e. the properties of the air layer between the contact surface and the outer shock, and the exhaust gas layer on the inside). Equations may be written for the total thickness, the mass flow in the air layer and exhaust layers and the total momentum.

They are:

$$\bar{\delta}_{ML} = \bar{\delta}_{JET,ML} + \bar{\delta}_{AIR,ML} \tag{56}$$

$$\frac{\dot{m}_{AIR,ML}}{\dot{m}_{JET}} = 2\,\bar{r}\,\bar{\delta}_{AIR,ML} \sin\theta \left(\frac{\gamma}{\gamma-1}\right)_{AIR,ML} \left(\frac{P_{AIR,ML}}{q_o}\right) \cdot \left(\frac{V_M^2}{h_{AIR,ML}}\right) \left(\frac{V_{AIR,ML}}{V_M}\right) \frac{1}{\mu\left(\gamma_j\right)} \tag{57}$$

$$\frac{\dot{m}_{JET,ML}}{\dot{m}_{JET}} = 2\,\bar{r}\,\bar{\delta}_{JET,ML} \sin\theta \left(\frac{\gamma}{\gamma-1}\right)_{JET,ML} \left(\frac{P_{JET,ML}}{q_o}\right) \cdot \left(\frac{V_M^2}{h_{JET,ML}}\right) \left(\frac{V_{JET,ML}}{V_M}\right) \frac{1}{\mu\left(\gamma_j\right)} \tag{58}$$

$$\left(\frac{\dot{m}_{ML}}{\dot{m}_{JET}}\right)\left(\frac{V_{ML}}{V_M}\right) = \left(\frac{\dot{m}_{JET,ML}}{\dot{m}_{JET}}\right)\left(\frac{V_{JET,ML}}{V_M}\right) + \left(\frac{\dot{m}_{AIR,ML}}{\dot{m}_{JET}}\right)\left(\frac{V_{AIR,ML}}{V_M}\right) \tag{59}$$

Where

$$\bar{\delta}_{AIR,ML} = \left(\frac{q_o}{P_c}\right)^{1/2} \frac{\delta_{AIR,ML}}{y^*} \tag{60}$$

$h_{AIR,ML}$ static enthalpy of air layer.

$$\mu\left(\gamma_j\right) = \frac{\dot{m}_{JET}\, V_M}{\pi\, y^{*2}\, P_c} = \sqrt{\frac{2\gamma_{JET}}{\gamma_{JET}^2 - 1}} \left(\frac{2}{\gamma_{JET}+1}\right)^{\frac{1}{\gamma_{JET}-1}} \tag{61}$$

There are four equations with four unknowns

$$\overline{\delta}_{JET,ML}\ ,\ \overline{\delta}_{AIR,ML}\ ,\ \frac{V_{AIR,ML}}{V_M}\ \text{and}\ \frac{V_{JET,ML}}{V_M}$$

The left hand sides are all known. The densities on the right are obtainable from the pressure and enthalpy by using an averaged equation of state for each layer.

$$\rho_{AIR,ML} = \left(\frac{\gamma}{\gamma-1}\right)_{AIR,ML} \frac{P_{AIR,ML}}{h_{AIR,ML}} \tag{62}$$

$$\rho_{JET,ML} = \left(\frac{\gamma}{\gamma-1}\right)_{JET,ML} \frac{P_{JET,ML}}{h_{JET,ML}} \tag{63}$$

where

$$\left(h_o\right)_{AIR,ML} = h_{AIR,ML} + \frac{V^2_{AIR,ML}}{2} = \frac{V_o^2}{2} \tag{64}$$

$$\left(h_o\right)_{JET,ML} = h_{JET,ML} + \frac{V^2_{JET,ML}}{2} = \frac{V_M^2}{2} \tag{65}$$

Solving Equation (56) through (59), $\left(V_{AIR,ML}/V_M\right)$ is found to be represented by a solution to a cubic equation:

$$\left(\frac{V_{AIR,ML}}{V_M}\right)^3 + \frac{A+B+C}{D}\left(\frac{V_{AIR,ML}}{V_M}\right)^2 + \frac{E+F+G+H}{D} \cdot \left(\frac{V_{AIR,ML}}{V_M}\right) + \frac{I}{D} = 0$$

where

$$A = 2\, a_1 a_3 c_2 b_3$$

$$B = \bar{\delta}_{ML}\, a_1 a_2 b_3$$

$$C = a_2 a_3 c_1$$

$$D = b_3 \left[a_1 b_3 c_2 + c_1 a_2 \right]$$

$$E = a_1 a_3^2 c_2$$

$$F = \bar{\delta}_{ML}\, a_1 a_2 a_3$$

$$G = -a_1 b_2^2 c_2$$

$$H = -a_2 b_1^2 b_3 c_1$$

$$I = -a_2 a_3 b_1^2 c_1$$

and

$$a_1 = 4\, \bar{r} \sin\theta \left(\frac{\gamma}{\gamma - 1} \right)_{AIR,\,ML} \left(\frac{P_{AIR,\,ML}}{q_o} \right) \frac{1}{\mu\left(\gamma_j\right)}$$

$$a_2 = 4\, \bar{r} \sin\theta \left(\frac{\gamma}{\gamma - 1} \right)_{JET,\,ML} \left(\frac{P_{JET,\,ML}}{q_o} \right) \frac{1}{\mu\left(\gamma_j\right)}$$

$$a_3 = \left(\frac{\dot{m}_{ML}}{\dot{m}_{JET}} \right) \left(\frac{V_{ML}}{V_M} \right) \left(\frac{\dot{m}_{JET}}{\dot{m}_{JET,\,ML}} \right)$$

$$b_1 = V_\infty / V_M$$

$$b_2 = 1$$

$$b_3 = - \left(\frac{\dot{m}_{AIR,\,ML}}{\dot{m}_{JET}} \right) \left(\frac{\dot{m}_{JET}}{\dot{m}_{JET,\,ML}} \right)$$

$$c_1 = \left(\frac{\dot{m}_{AIR,ML}}{\dot{m}_{JET}} \right)$$

$$c_2 = \left(\frac{\dot{m}_{JET,ML}}{\dot{m}_{JET}} \right)$$

With $(V_{AIR,ML}/V_M)$ determined, solutions for the other unknowns may now be obtained.

This technique has been used to determine the characteristics of the overall and individual layers for a typical plume (γ_{ML} = 1.325, M_{exit} = 3.0 and γ_{JET} = 1.25). The ratio of specific heats for overall layer was assumed to be the average of the air and exhaust gas layers.

The variation of the total thickness of the air-exhaust gas layer with forward speed ratio is shown in Figure 14. A comparison of the total layer thickness (Figure 14) with the exhaust layer thickness (Figure 15) for a V_∞/V_M ratio near unity indicates the individual layers are nearly the same thickness. For larger V_∞/V_M ratios, the exhaust layer becomes much thicker than the air layer. The average pressure in the air-exhaust gas layer is noted in Figure 16. The mass flow in the overall layer and the mass flow in the exhaust gas layer are noted in Figures 17 and 18 respectively. Fifty percent of the mass flow exiting from the rocket engine is entrained in the exhaust gas layer, when the non-dimensional longitudinal distance, $\overline{X}$ equals 1.2. The average static enthalpy of the overall layer and the density in the exhaust layer are shown in Figures 19 and 20. The magnitude of the density in the exhaust gas layer relative to the exit plane density may be determined from Figure 20 if the dynamic pressure q_o, the engine chamber pressure P_c and expansion ratio are known. If frozen flow is assumed from the engine exhaust plane through the exhaust gas layer, the average electron density in the exhaust layer is also determined. In addition, since the average temperature in the exhaust gas layer is known, the layer collision frequency may be determined.

Calculations were performed for the case where the specific heat ratio for the overall layer is evaluated using the relative mass flow in the individual layers instead of assuming an average of the exhaust gas and air layer specific heat ratio, i.e.;

$$\gamma_{ML} = \frac{C_{AIR} C_{P_{AIR}} + C_{JET} C_{P_{JET}}}{C_{AIR} C_{V_{AIR}} + C_{JET} C_{V_{JET}}}$$

or

$$\gamma_{ML} = \frac{\left(\frac{\dot{m}_{AIR,ML}}{\dot{m}_{JET}}\right) C_{P_{AIR}} + \left(\frac{\dot{m}_{JET,ML}}{\dot{m}_{JET}}\right) C_{P_{JET}}}{\left(\frac{\dot{m}_{AIR,ML}}{\dot{m}_{JET}}\right)\left(C_{P_{AIR}} - R_{AIR}\right) + \left(\frac{\dot{m}_{JET,ML}}{\dot{m}_{JET}}\right)\left(C_{P_{JET}} - R_{JET}\right)}$$

The variable specific heat ratio calculations produced results substantially similar to the constant γ calculations. The variable γ calculations predicted slightly smaller magnitude for overall and individual layer thickness and slightly larger values for the density in the exhaust layer. The mass flow in the overall and individual layers was unaffected by the method used to calculate γ.

5. NEAR-FIELD SHOCK WAVES PRODUCED BY ROCKET PLUMES

The theory describing the far-field flow field about supersonic, axisymetric bodies was developed by G. B. Whitham (1952). This theory can be used to predict the location and strength of shock wave and the plume drag. Experimental agreement with the theory has been obtained by DuMond (1946) with bullets, Carlson (1959) in wind tunnel investigations and by Moglieri, (1959) and Mullen, (1956) in flight tests of full scale airplanes.

The Whitham theory is a modification of linearized supersonic flow theory which introduces shock waves by replacing the Mach lines of the linear theory with accurate expressions for the characteristics. The basic distributing function of the body shape remains unchanged.

The formulas predicting the location of the front shock wave, the pressure discontinuity, and the plume drag are

$$x - \beta r - y_o = -r^{1/4} \sqrt{2k \int_o^{y_o} F(y)\, d\, y} \tag{66}$$

$$\frac{\Delta P}{P_\infty} = \frac{2^{1/4}\, \gamma\, \beta^{1/4}}{\sqrt{\gamma+1}\; r^{3/4}} \sqrt{\int_o^{y_o} F(y)\, d\, y} \tag{67}$$

$$D = \rho_\infty V_\infty^2\, \pi \int_o^{y_o} F^2(y), d\, y \tag{68}$$

where $\beta \quad \sqrt{M^2 - 1}$

γ polytropic index

x, r cylindrical coordinates: x is measured along body axis downstream from the nose, r is the radial coordinate measured perpendicular to x.

M free stream Mach number

P pressure

D drag

$$k = \frac{M^4(\gamma + 1)}{\sqrt{2}\,\beta^{3/2}}$$

$$\Delta P = P - P_\infty$$

The basic function $F(\eta)$ is the shape integral of the plume defined as

$$F(y) = \frac{1}{2\pi} \int_o^y \frac{S''(\zeta)}{y-\zeta}\, d\zeta \tag{69}$$

where S is the cross-sectional area, πR^2. The value of the upper limit, y_o, is determined from the condition that the integral

$$I(y) = \int_o^y F(\eta)\, d\,\eta \tag{70}$$

be a maximum at $y = y_o$. A necessary condition for a maximum at $y = y_o$ is

$$\frac{dI}{dy} = F(y) = o \tag{71}$$

The Whitham theory is inapplicable to an elliptical body because of the blunt nose. However, experimental work, Carlson (1959), shows that the far-field pressures are essentially the same as those for a pointed parabolic body of the same fineness ratio. Thus instead of using the blunt elliptical plume shape specified as

$$R^2 = K_x \left(x - \frac{x^2}{2L} \right) \tag{72}$$

the plume will be described as a parabolic body having the same r_{max} as the ellipsoidal plume.

$$r = \sqrt{\frac{2K_x}{L}} \sqrt{x - \frac{x^2}{2L}} \tag{73}$$

Integrating Eq. (5.4), the shape integral is obtained as

$$F(y) = \frac{4K_x \sqrt{y}}{L} \left(1 - 2\,\frac{y}{L} + 0.8\,\frac{y}{L}^2\right) \tag{74}$$

The parameter in the shock wave pressure and position equations is given as

$$\int_o^{y_o} F(y)\, dy = 0.92\, K_x \sqrt{L}$$

where the upper limited is determined as $y_o = 0.692L$.

The accuracy of this approach can be determined by evaluating the plume drag using Whitham's theory (Eq. 68) and comparing the results with the known drag determined by Hill and Habert (1963). The drag obtained from Eq. (68) is

$$D = 0.45\pi\, \rho_\infty\, V_\infty^2\, K_x^2$$

The drag computed by the Whitham theory agrees to within 3 percent of the drag computed for the ellipsoid shape using the drag coefficients evaluated by Hill and Habert (1963). The comparison is made at $M_\infty = 10$ on a representative trajectory.

A wind tunnel test at Mach number 2.01 is available (Carlson 1959) which gives direct comparison between the experiments with an ellipsoid shape and the theory for the equivalent parabolic body. The comparison is shown in Figure 21.

The plume shock wave position and strength can now be described as

$$x - \beta r - 0.69\,L = r^{1/4}\sqrt{1.83\,k\,K_x\sqrt{L}}$$

$$\frac{\Delta P}{P_\infty} = \frac{1.03\,\beta^{1/4}}{r^{3/4}}\sqrt{K_x\sqrt{L}}$$

The shockwave overpressure has been calculated for the Saturn and Atlas second stage rockets and is shown in Table 5.1. The radial distance from the flight path to the point of ten percent overpressure is given, neglecting atmospheric attenuation of the shockwave. The above expression describes the shockwave to the point it decays into an acoustic wave. Thereafter, the acoustic disturbance must be treated by taking into account the variation in atmospheric transport properties using ray tracing methods or specifying the technique developed by Meyer (1962). The near-field model describing shock waves of strength, $\Delta P/P_\infty > 0.1$, is valid for distance up to 50-100 km from the plume (see Table 5.1).

TABLE 5.1

NUMERICAL RESULTS

	Saturn				Atlas			
Altitude	K_x	L	$\frac{\Delta P}{P_\infty} r^{3/4}$	r at $\frac{\Delta P}{P_\infty} = .1$	K_x	L	$\frac{\Delta P}{P_\infty} r^{3/4}$	r at $\frac{\Delta P}{P_\infty} = .1$
110	.35	9.1	1.88	50	.24	7.15	1.46	35
130	1.25	22.5	3.95	137	.81	17.6	3.13	90

Note: All dimensions in kilometers.

6. SUMMARY AND CONCLUSIONS

Theoretical models are described which provide an improved analytic description of the gas dynamics of high altitude rocket plumes. These methods are:

1. A simple analytic description of the exhaust flow from rocket motors into the region bounded by the inner shock wave and Mach disc.
2. A model for the two phase flow in the exhaust of solid propellant rocket vehicles and the effect of such flow on the resulting plume characteristics.
3. An analytic description of the flow properties in the air-exhaust gas layer on the periphery of the rocket plume.

The results described in this report in conjunction with those previously developed by Hill et al and Alden et al allow the overall features of plumes from both liquid and solid propellant rocket vehicles to be described.

In addition the structure of plumes has been described in sufficient detail to allow an ionization model for high altitude rocket plumes to be constructed. Such a model is described in an Addendum to this report.

7. REFERENCES

Alden, H. L., and Habert, R. H., "Gas Dynamics of High-Altitude Rocket Plumes", MITHRAS Report MC 63-80-R1, July 1964.

Altshuler, S., Moe, M. M., and Molund, P., "The Electromagnetics of the Rocket Exhaust", GM-TR-0165-00397, STL Inc., 15 June 1958.

Carlson, Harry W., "An Investigation of Some Aspects of the Sonic Boom by Means of Wind-Tunnel Measurements of Pressures About Several Bodies at a Mach Number of 2.01", NASA TN D-161, 1959.

DuMond, Jesse W. M., Cohen, E. Richard, Panofsky, W. K. H., and Deeds, Edward, " A Determination of the Wave Forms and Laws of Propagation and Dissipation of Ballistic Shock Waves". Jour. Acous. Soc. of America, Vol. 18, No. 1, July 1946.

Hill, J. A. F., and Habert, R. H., "Gas Dynamics of High-Altitude Missiles Trails", MITHRAS Report MC 61-18-R1, January 1963.

Maglieri, Domenic, J., Hubbard, Harvey H., and Lansing, Donald L., "Ground Measurements of the Shock-Wave Noise from Airplanes in Level Flight at Mach Numbers to 1.4 and at altitudes to 45,000 Feet". NASA TN D-48, 1959.

Meyer, Richard E. (1962), "On the Far Field of a Body Rising Through the Atmosphere", J. Geophysics Res. 67, 2361-2366.

Mullens, Marshall E., "A Flight Test Investigation of the Sonic Boom". AFFTC-TN-56-20, Air Res. and Dev. Command, U. S. Air Force, May 1956.

Sibulkin, M., and Gallaher, W. H., "Far Field Approximation for a Nozzle Exhausting into a Vacuum", AIAA J., Vol. 1, No. 6, June 1963, p. 1452 - 1453.

Wang, C. J., Peterson, J. B. and Anderson, R., "Gas Flow Tables", Space Technology Laboratories, Inc., GM-TR-154, March (1957).

Whitham, G. B., "The Flow Pattern of a Supersonic Projectile". Communications on Pure and Appl. Math., Vol. V, No. 3, Aug. 1952.

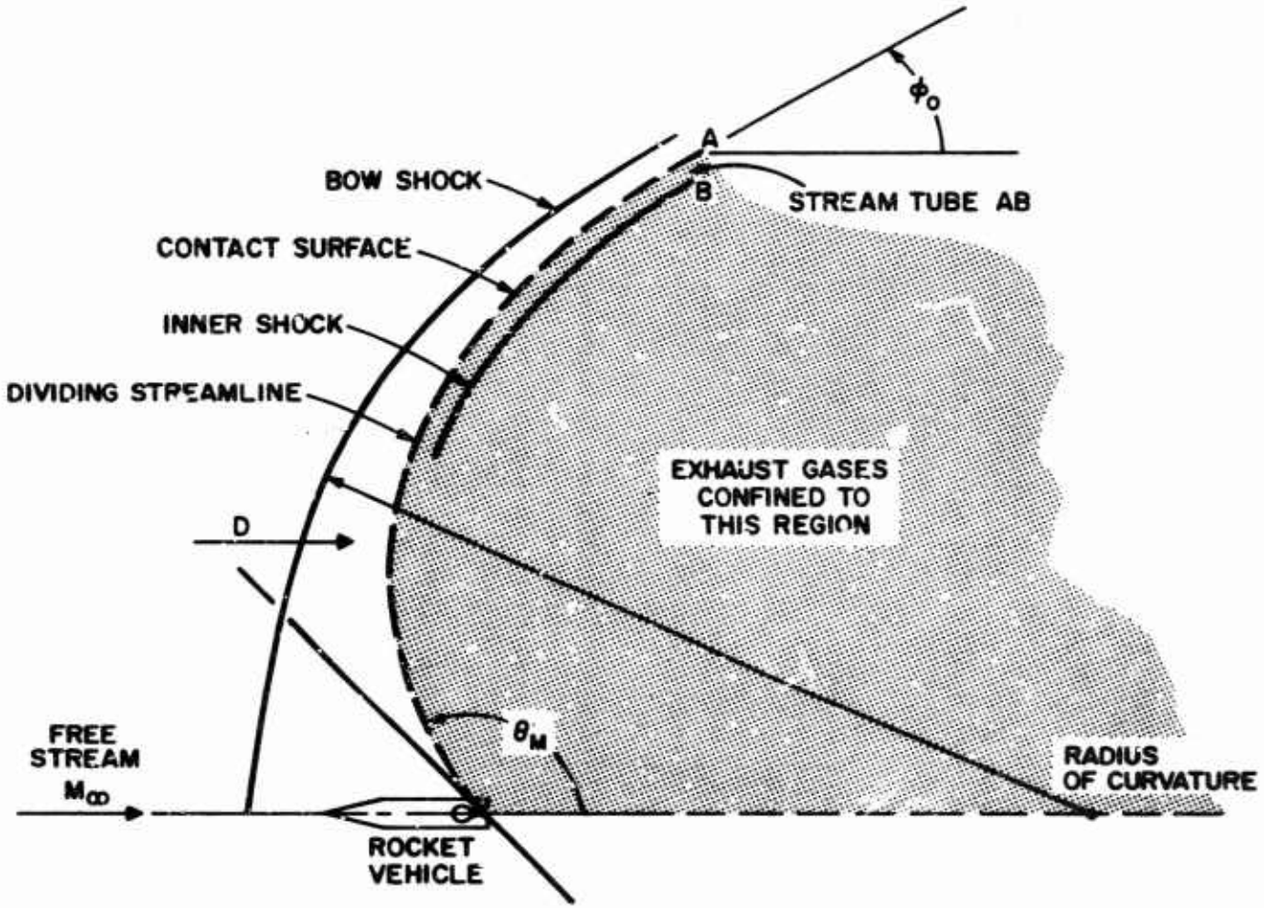

Figure 1. Structure of high altitude plume.

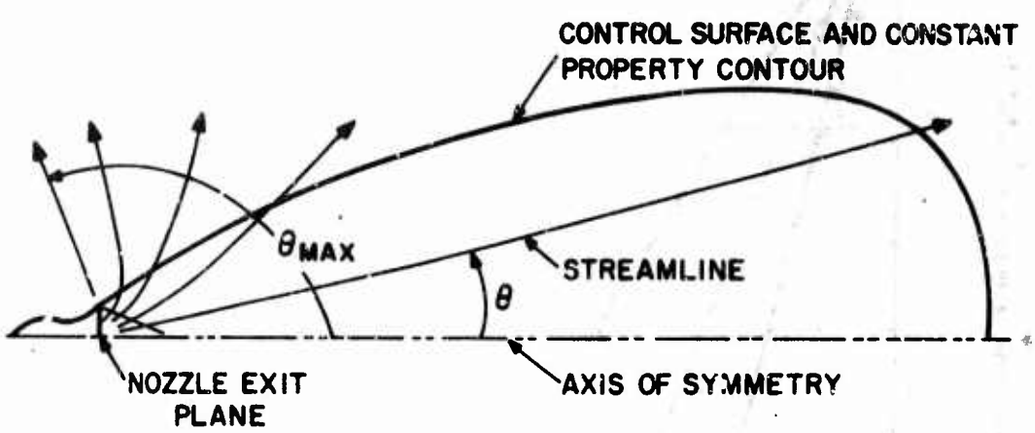

Figure 2. Schematic flow pattern of nozzle exhausting into a vacuum.

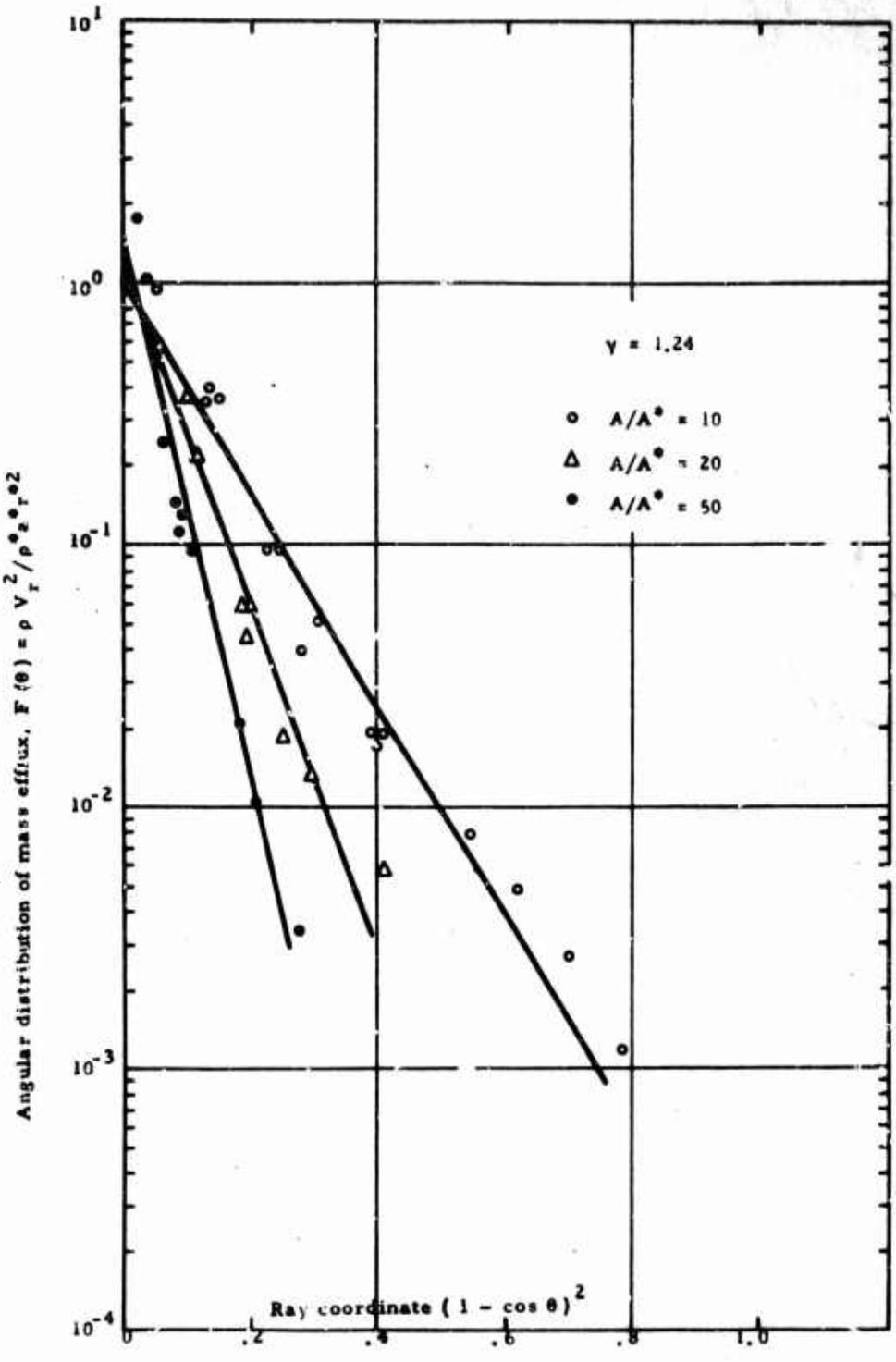

Figure 3. Expansion of three plumes with γ = 1.24.

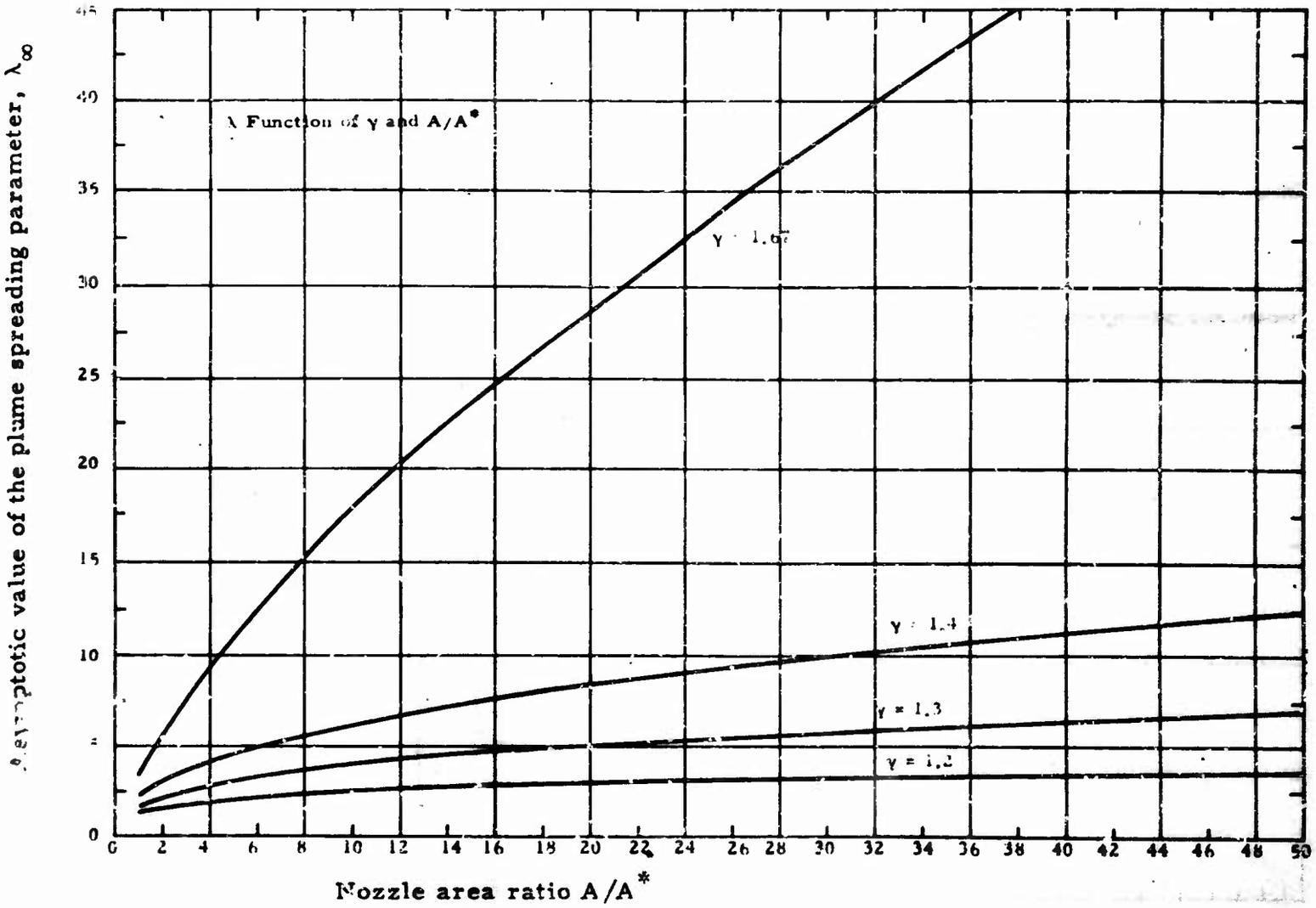

Figure 4. Variation of λ_∞ with nozzle area ratio.

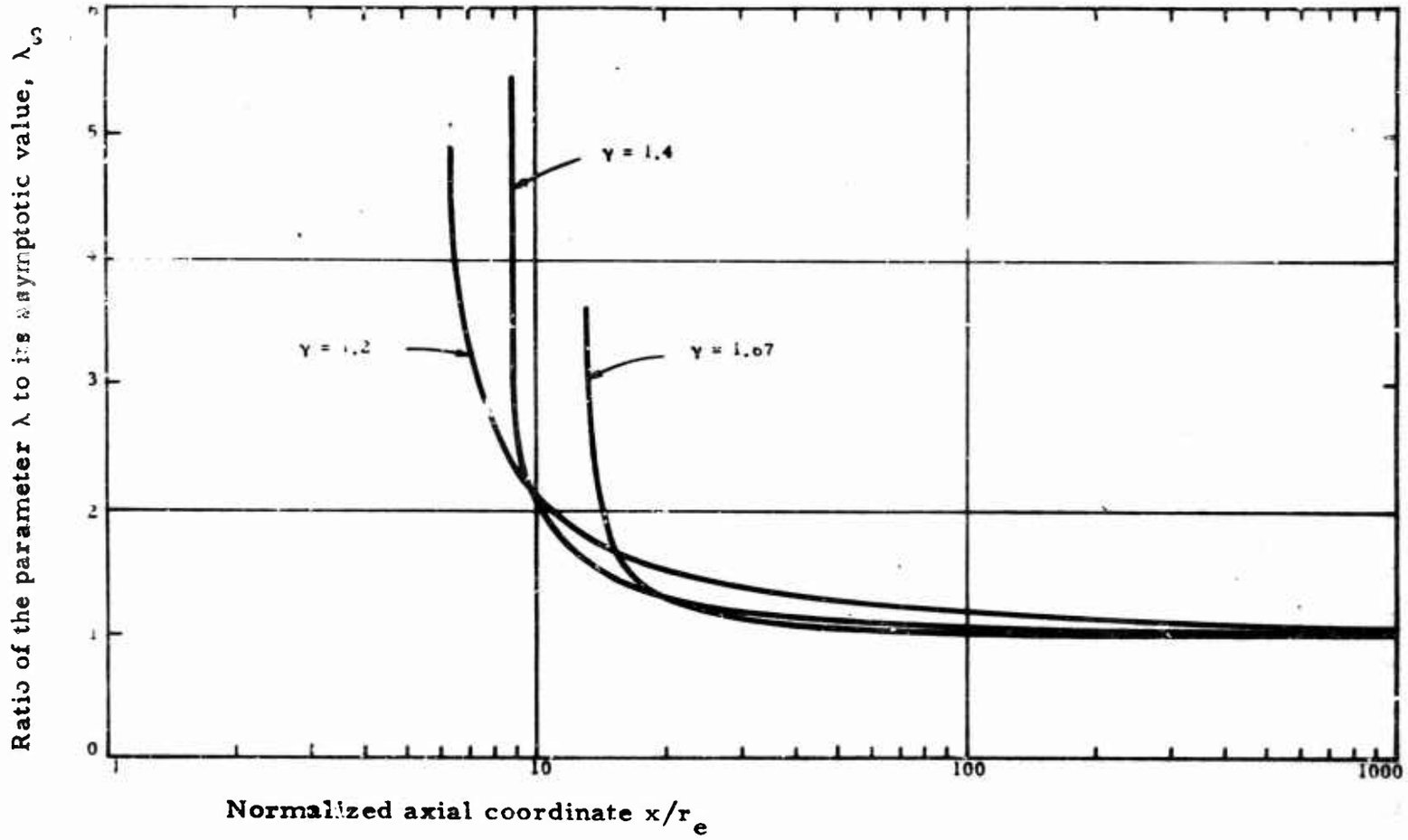

Figure 5. Variation of λ along plume with A/A* = 25.

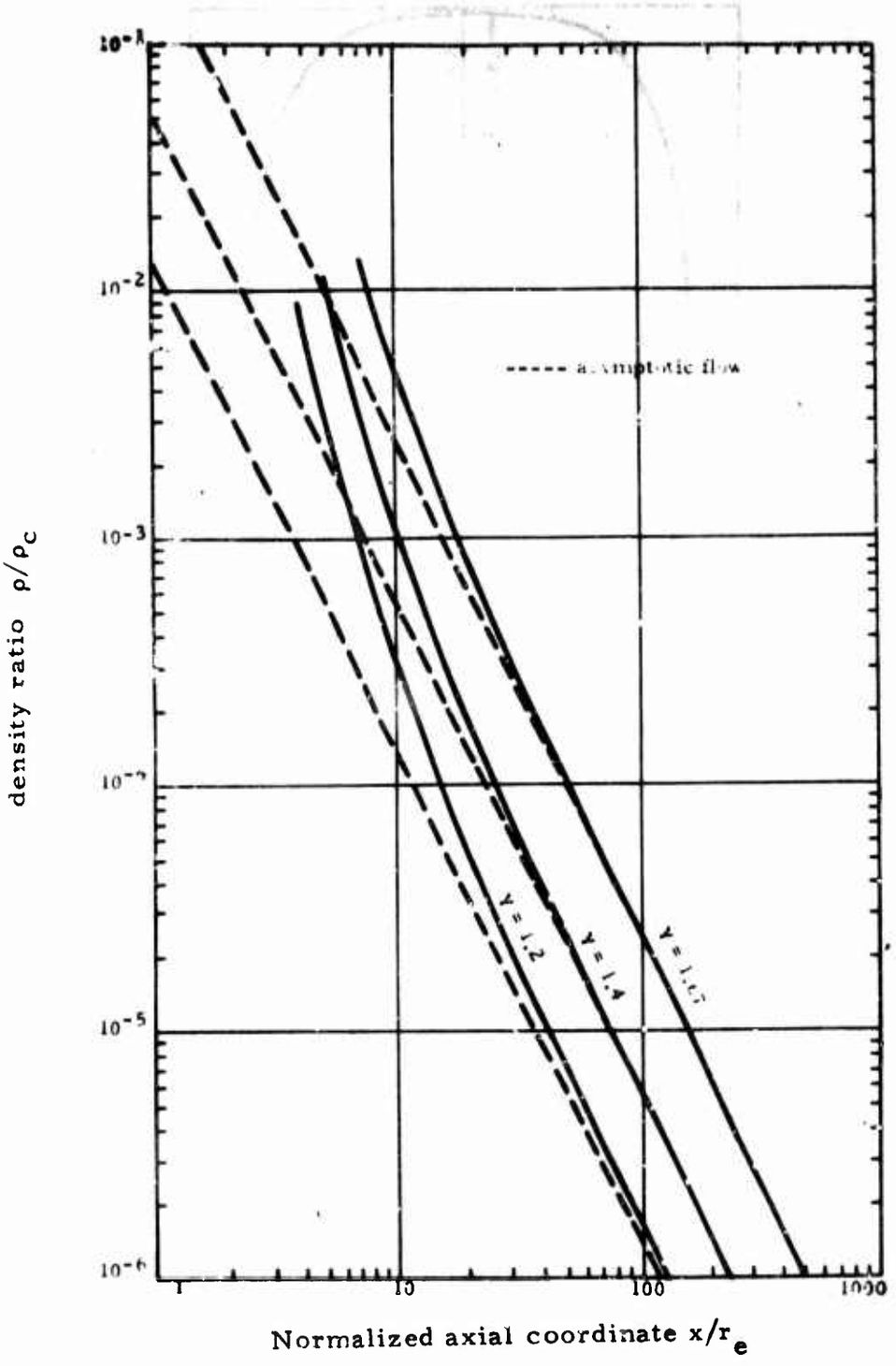

Figure 6. Axial density decay for A/A* = 25.

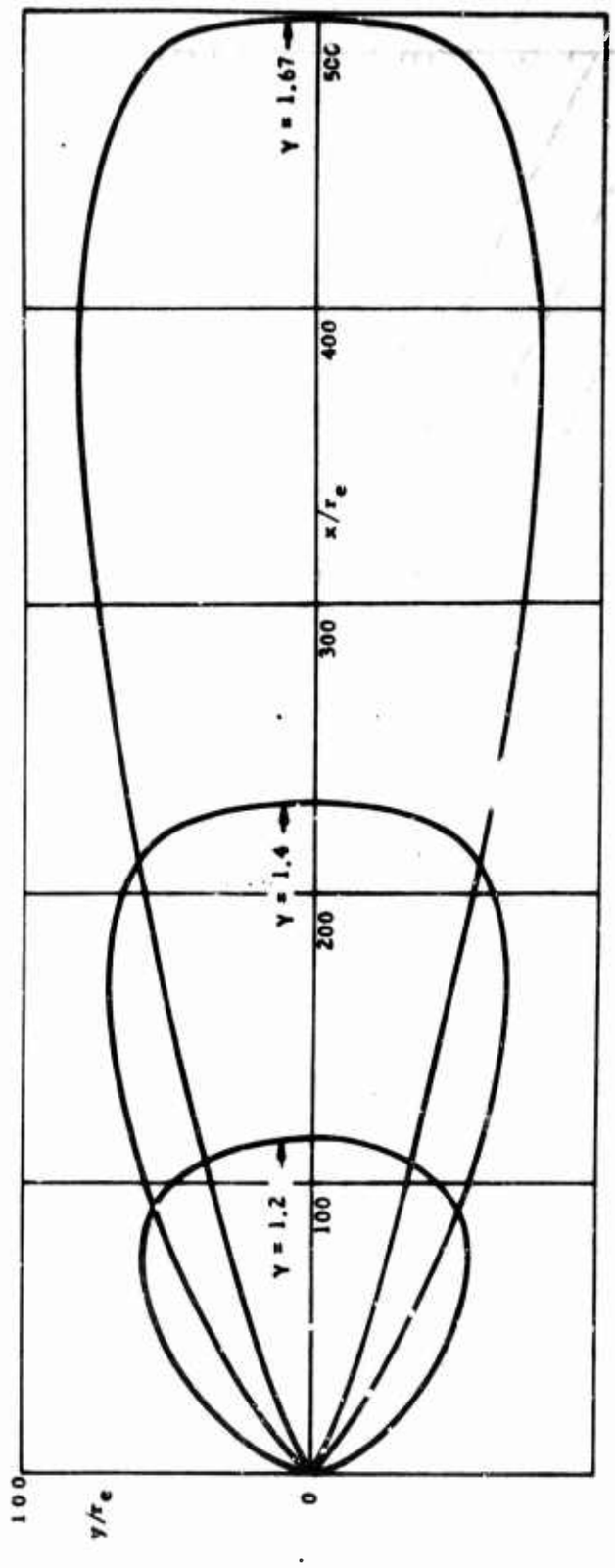

Figure 7. Contours of constant density ratio $\rho/\rho_c = 10^{-6}$.

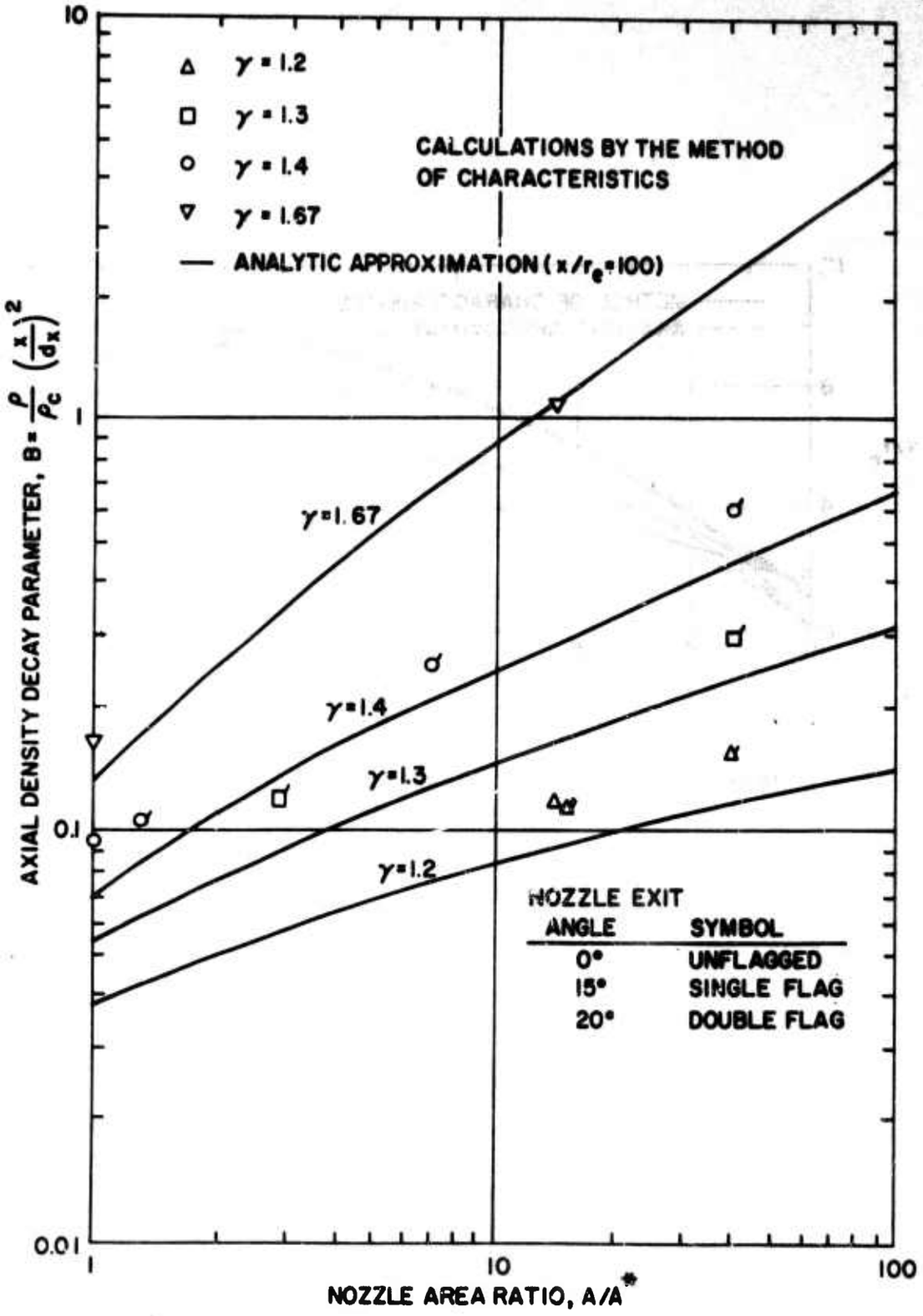

Figure 8. "Exact" and approximate calculations of density decay along plume axis.

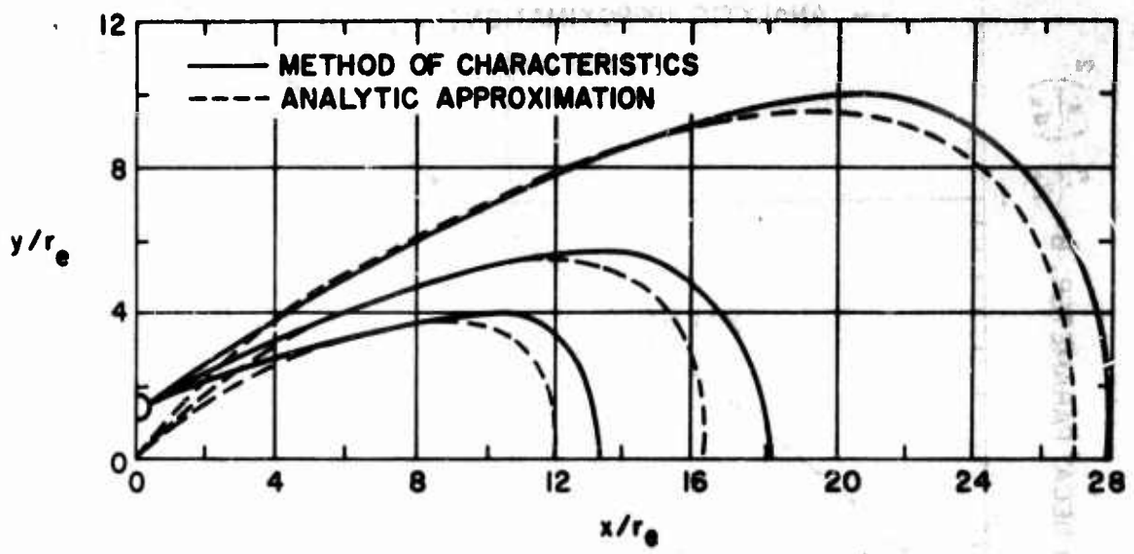

Figure 9. "Exact" and approximate constant-density contours for $A/A^* = 25$; $\gamma = 1.29$.

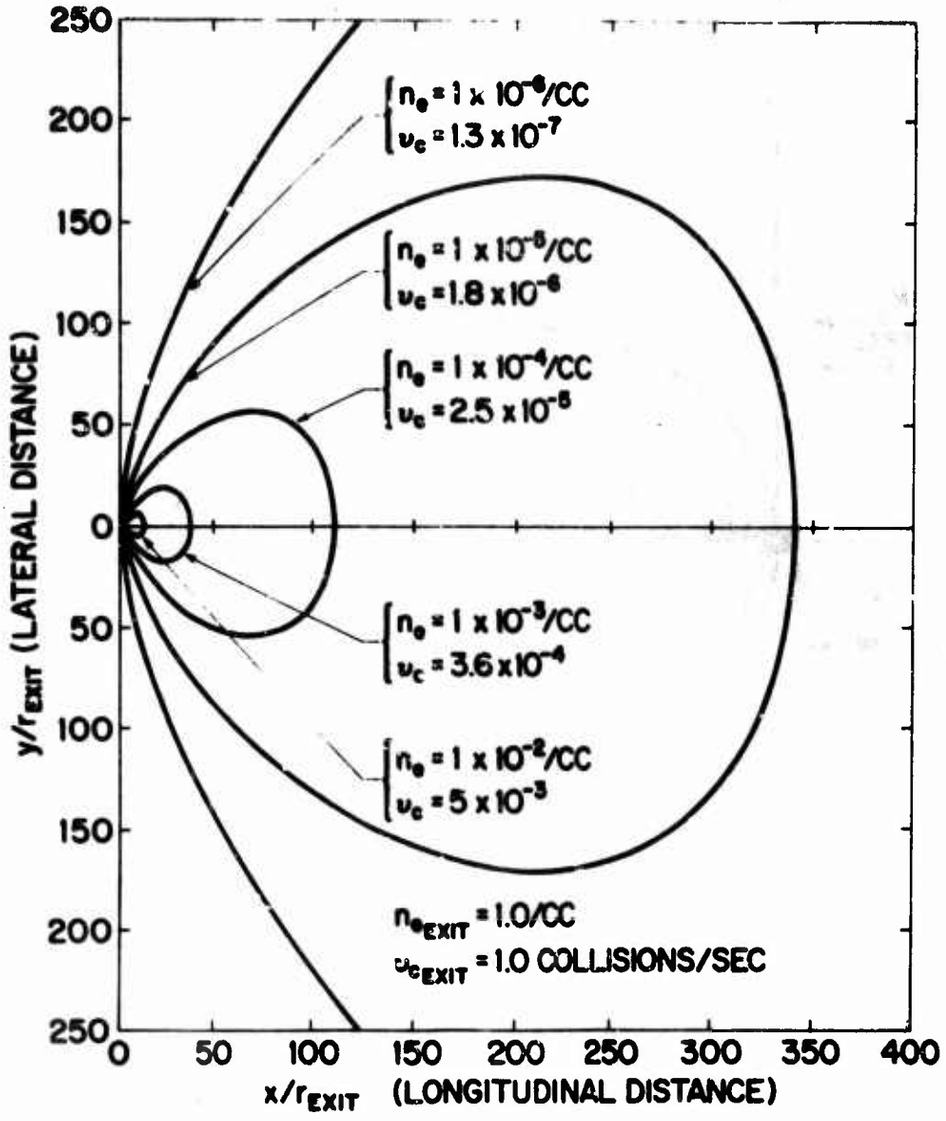

Figure 10. Electron density contours.

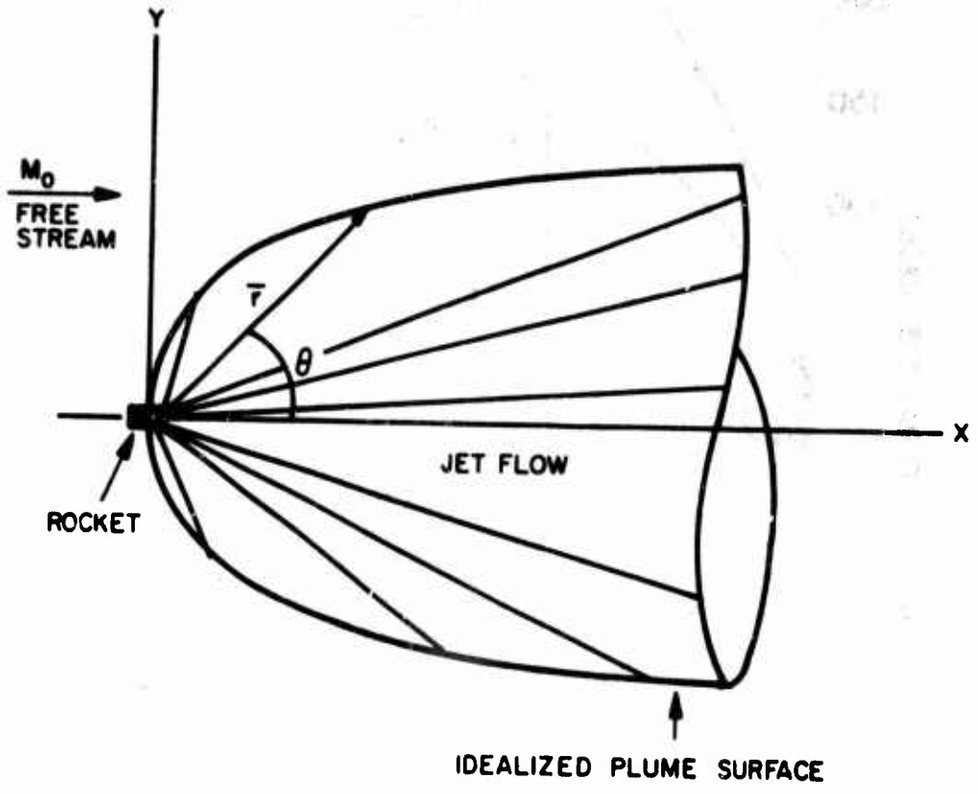

Figure 11. Coordinates for calculation of idealized plume surface.

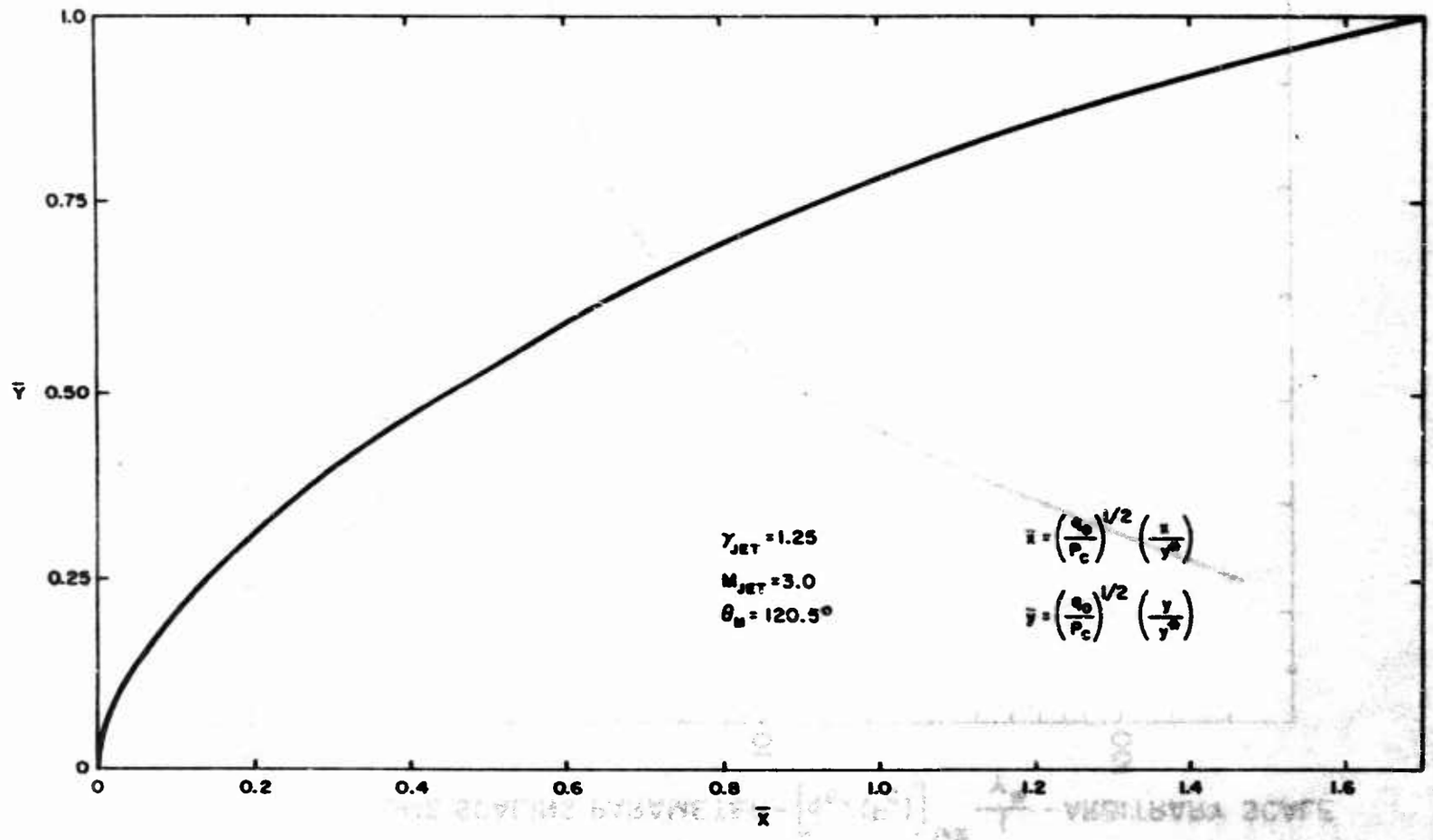

Figure 12. Plume contact surface location.

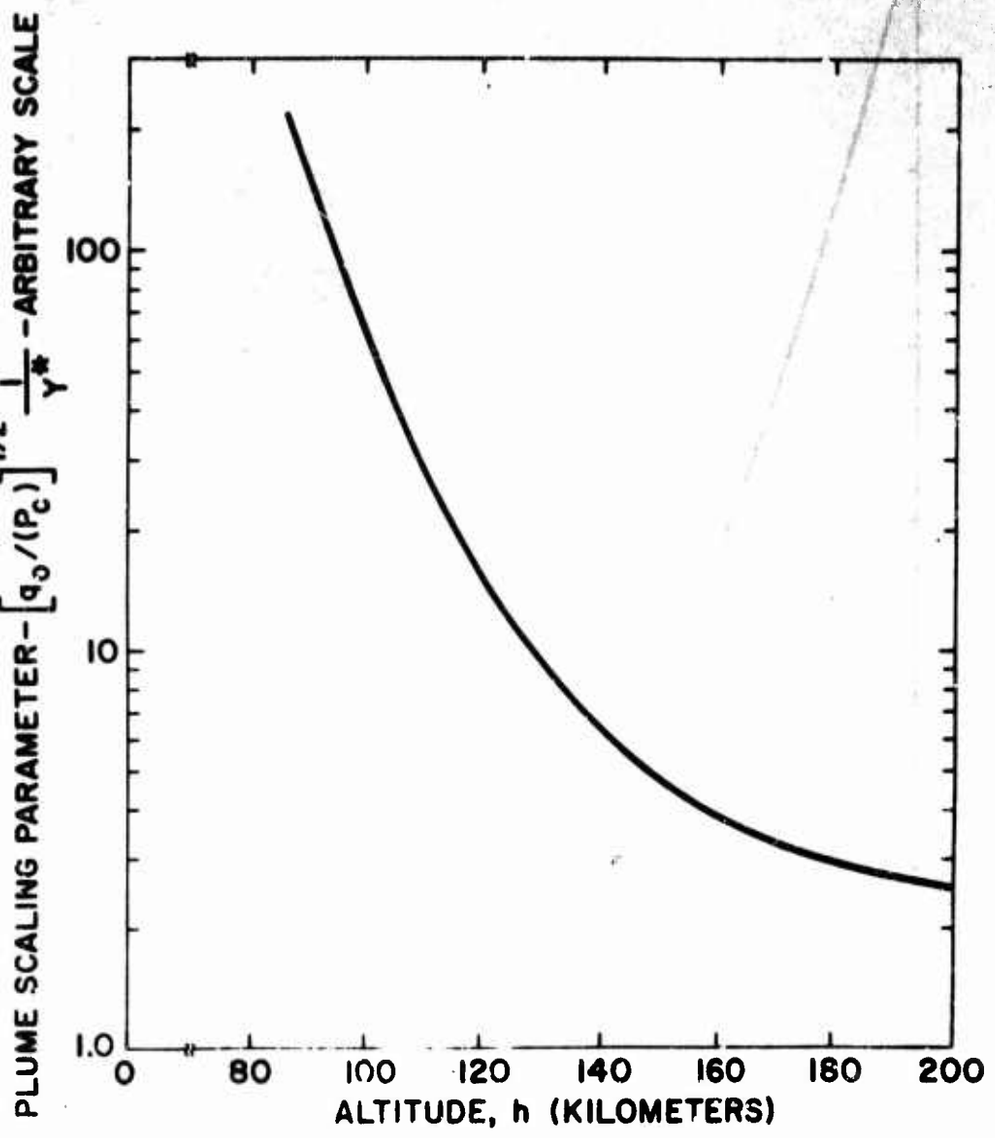

Figure 13. Plume scaling parameter.

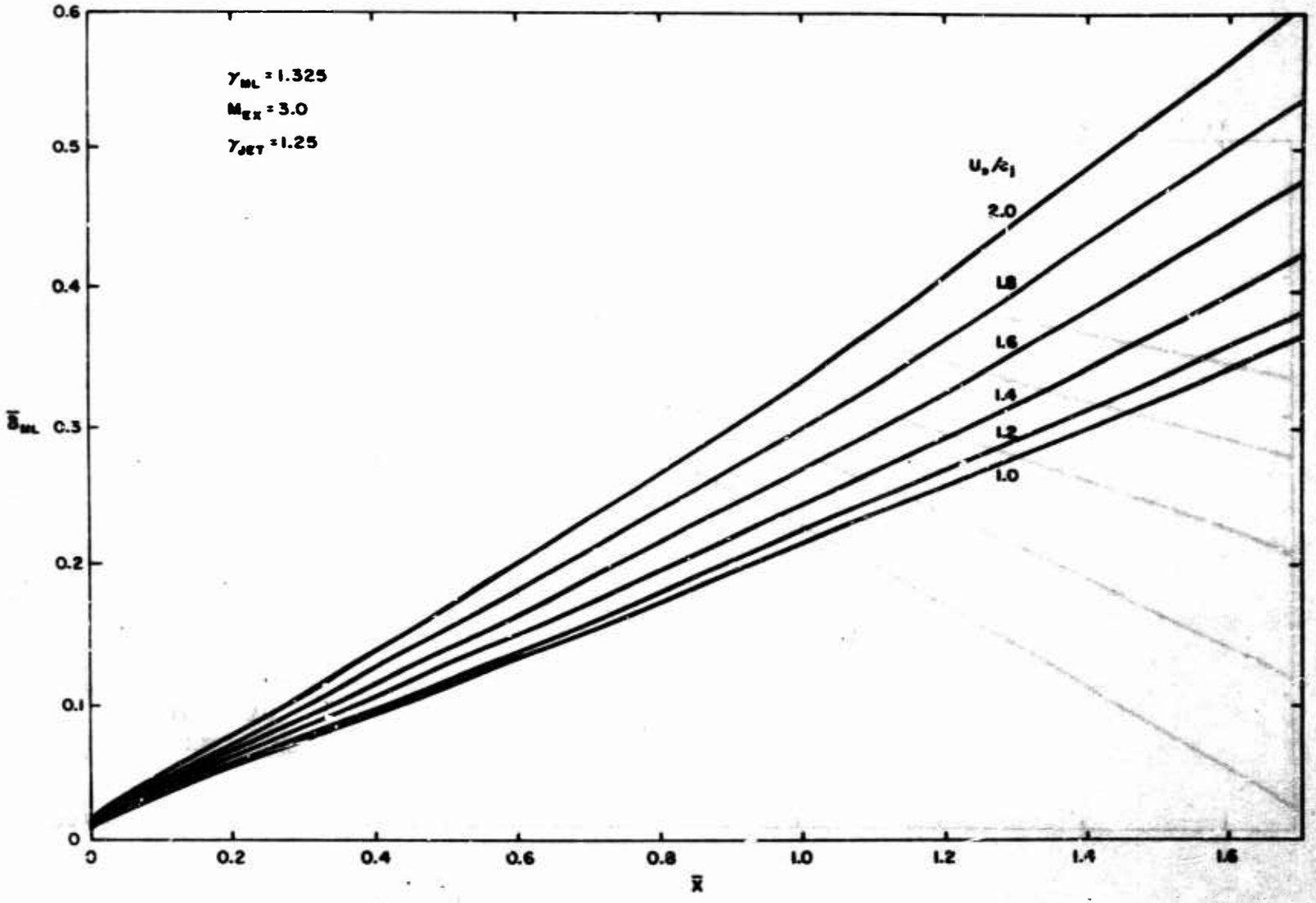

Figure 14. Total thickness of air-exhaust gas layer.

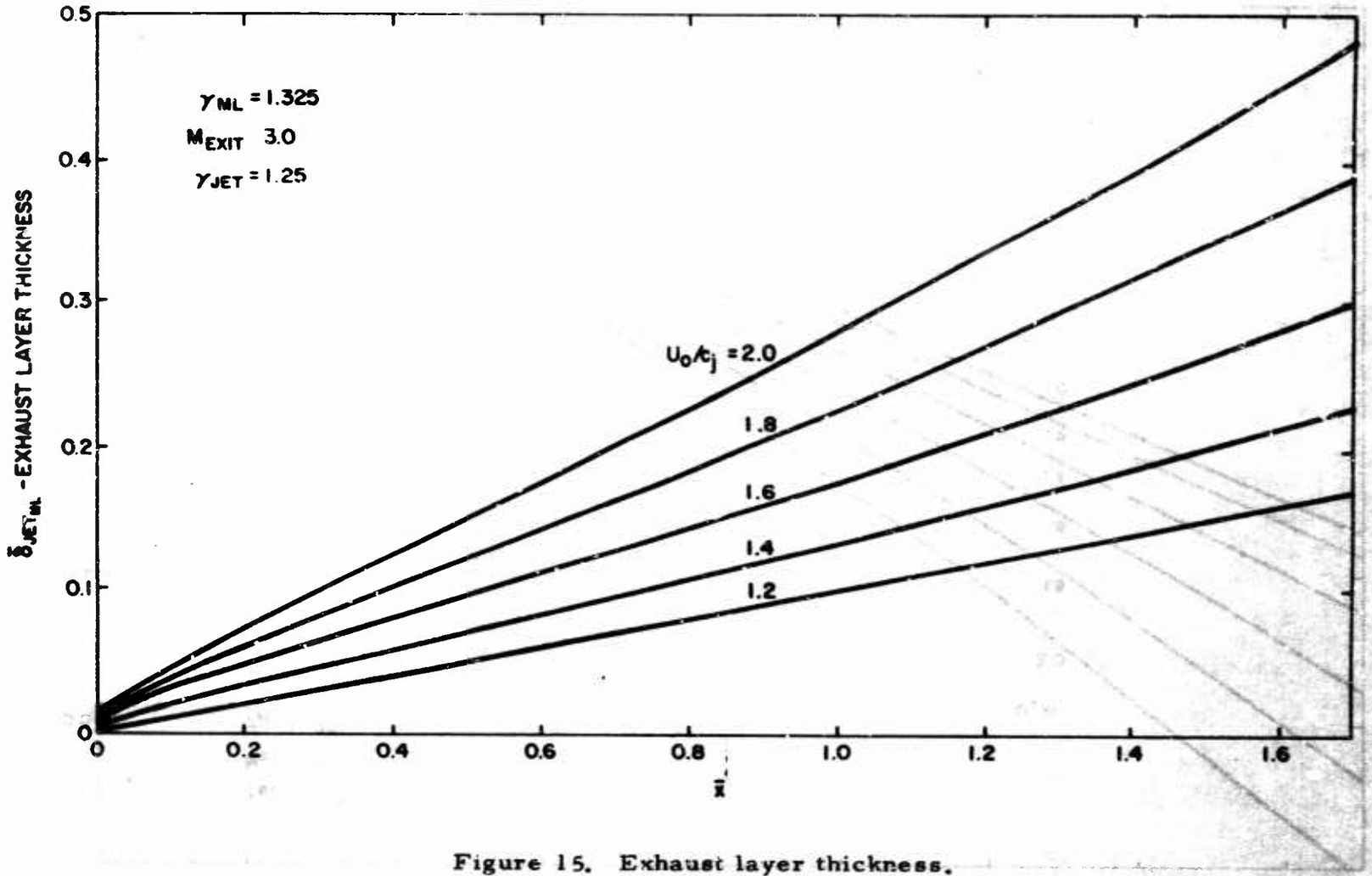

Figure 15. Exhaust layer thickness.

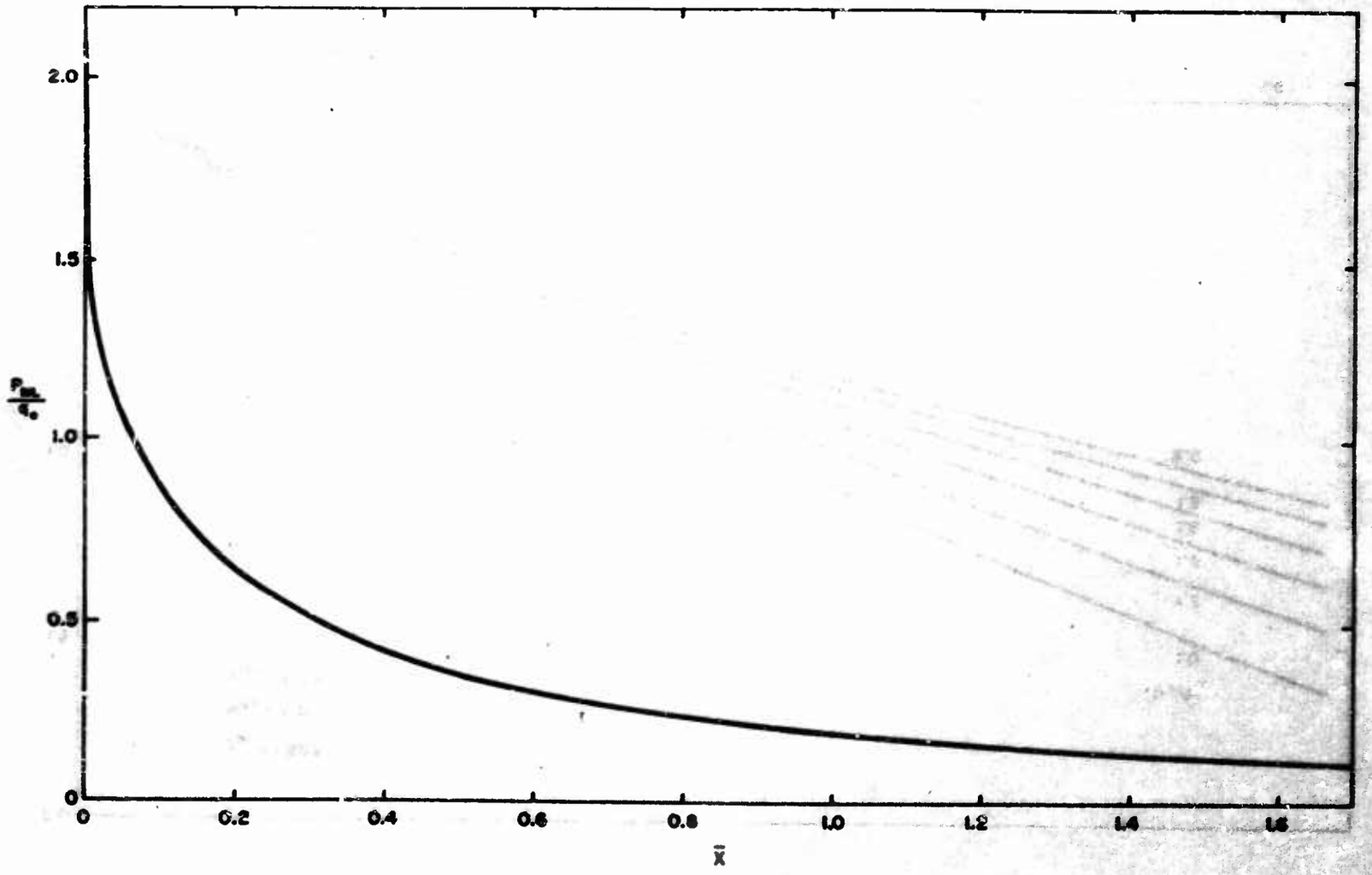

Figure 16. Average pressure in air-exhaust gas layer.

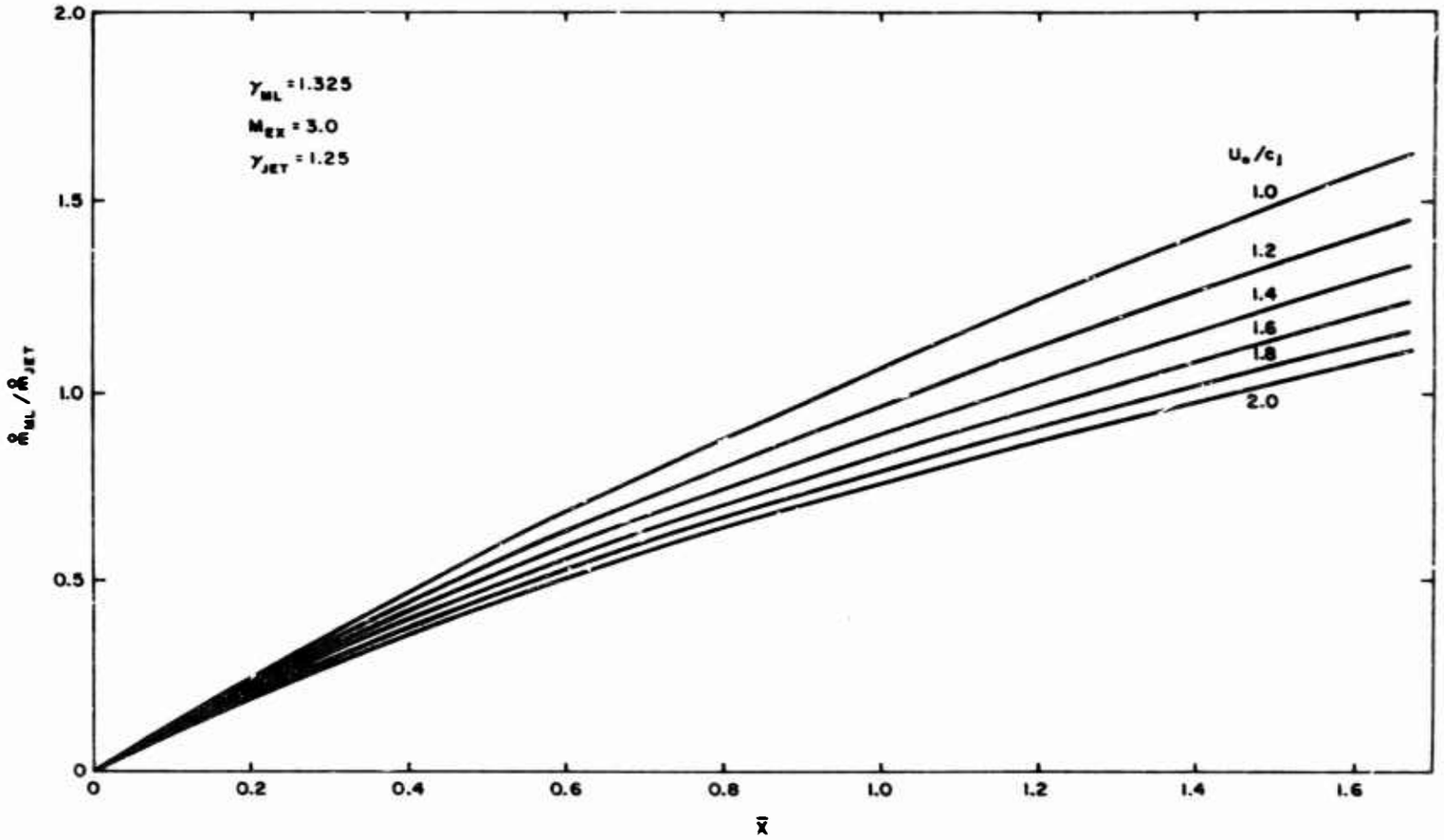

Figure 17. Mass flow in air-exhaust gas layer.

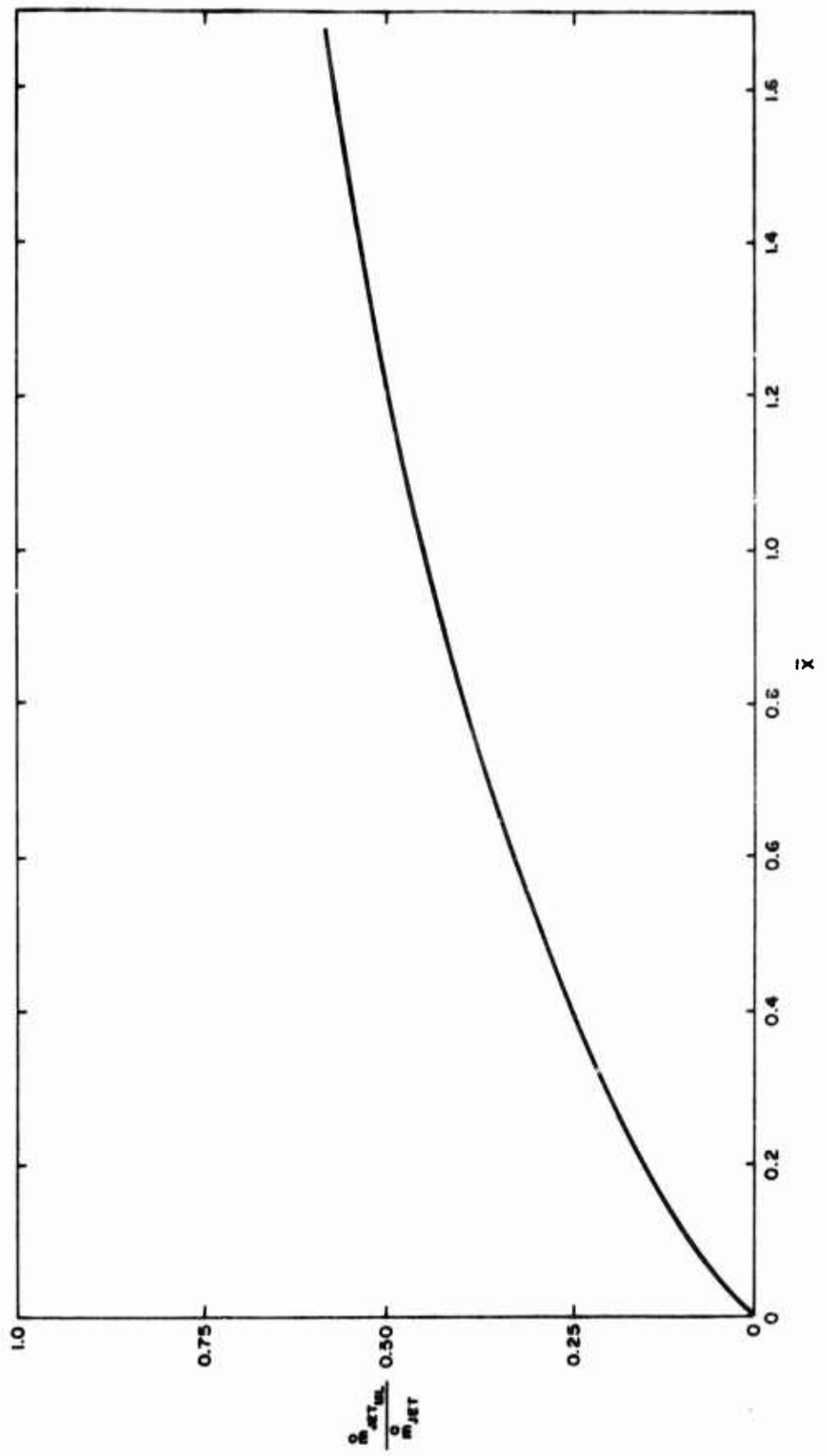

Figure 18. Mass flow in exhaust gas layer.

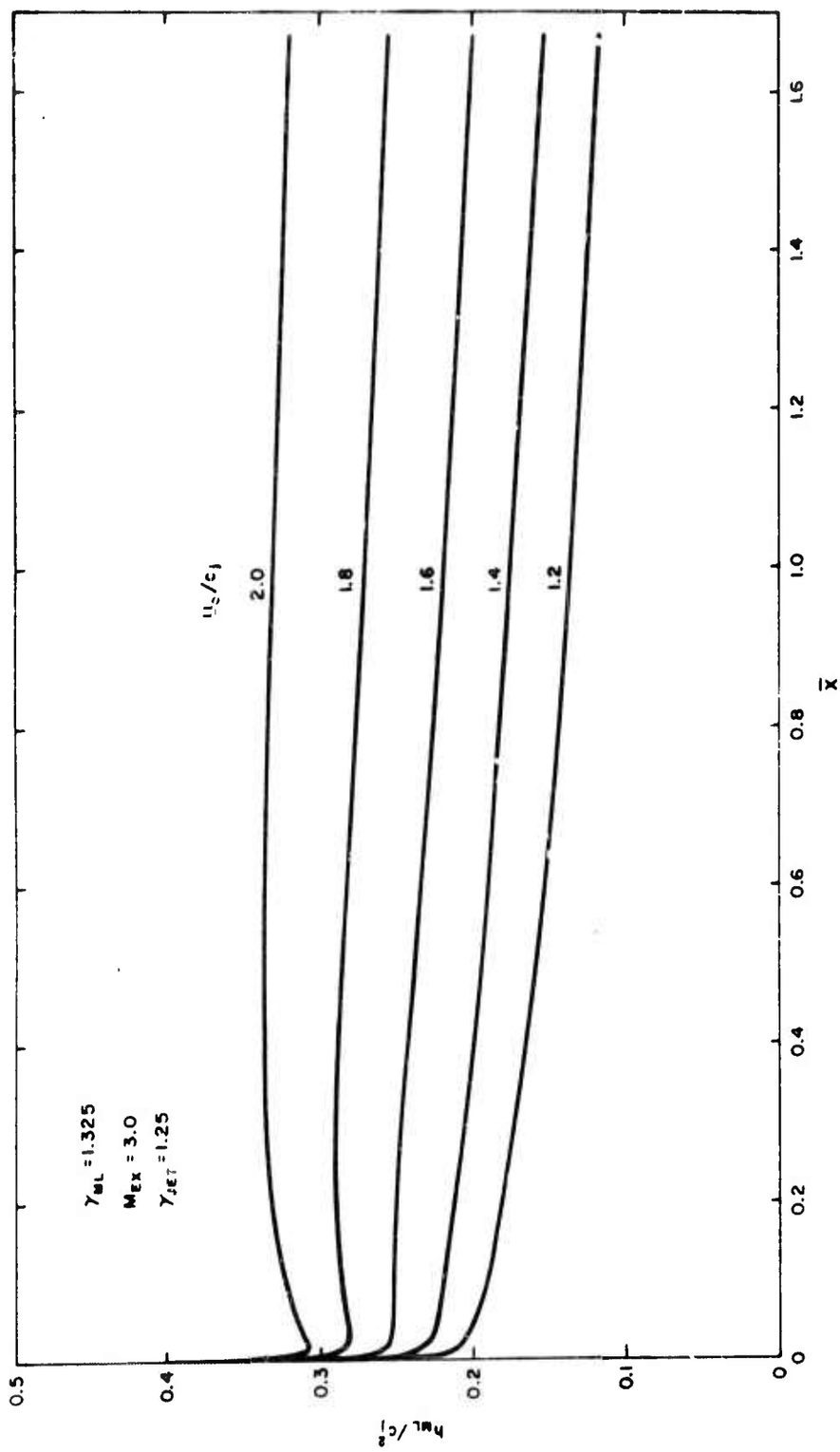

Figure 19. Average enthalpy in air-exhaust gas layer.

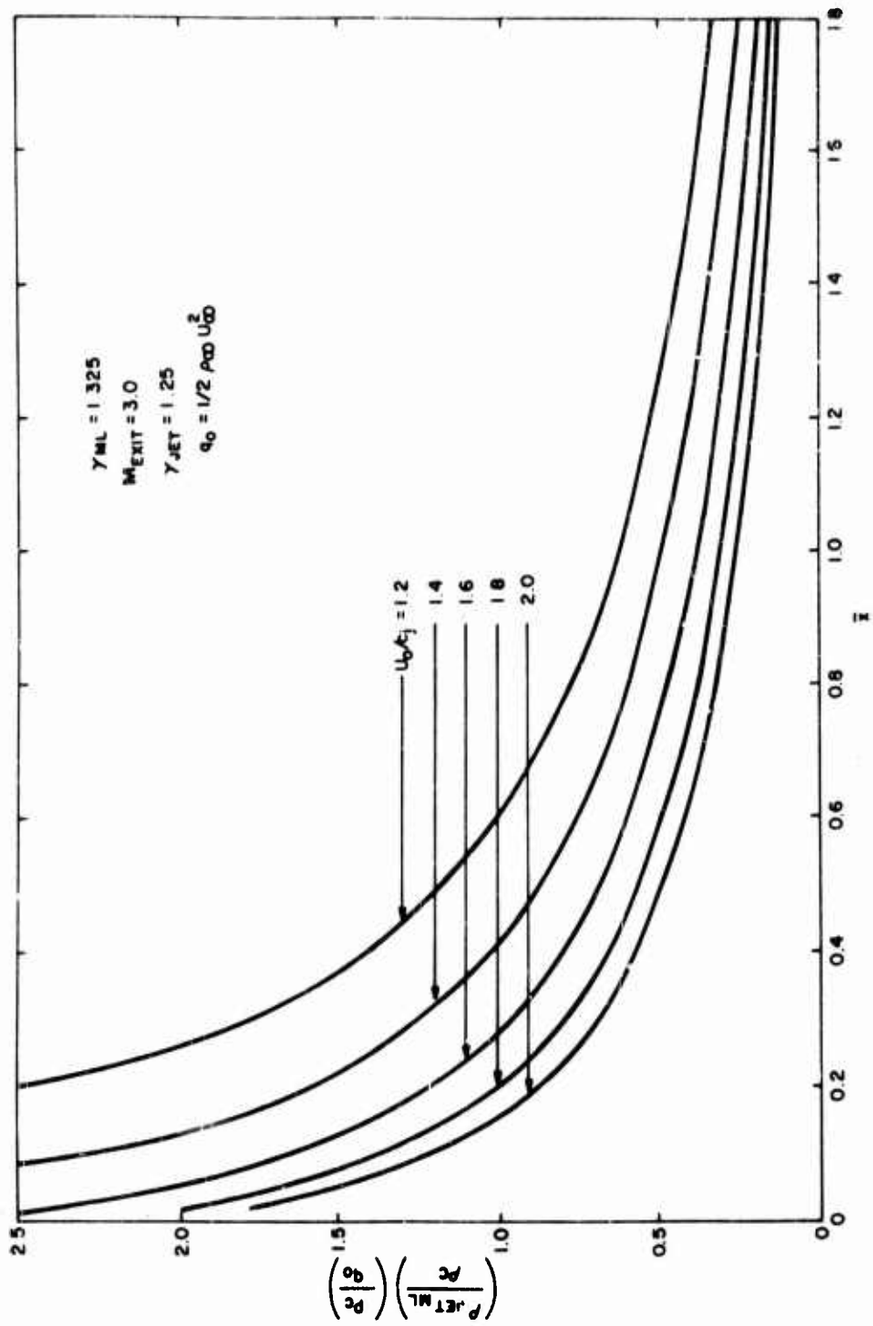

Figure 20. Density of exhaust layer.

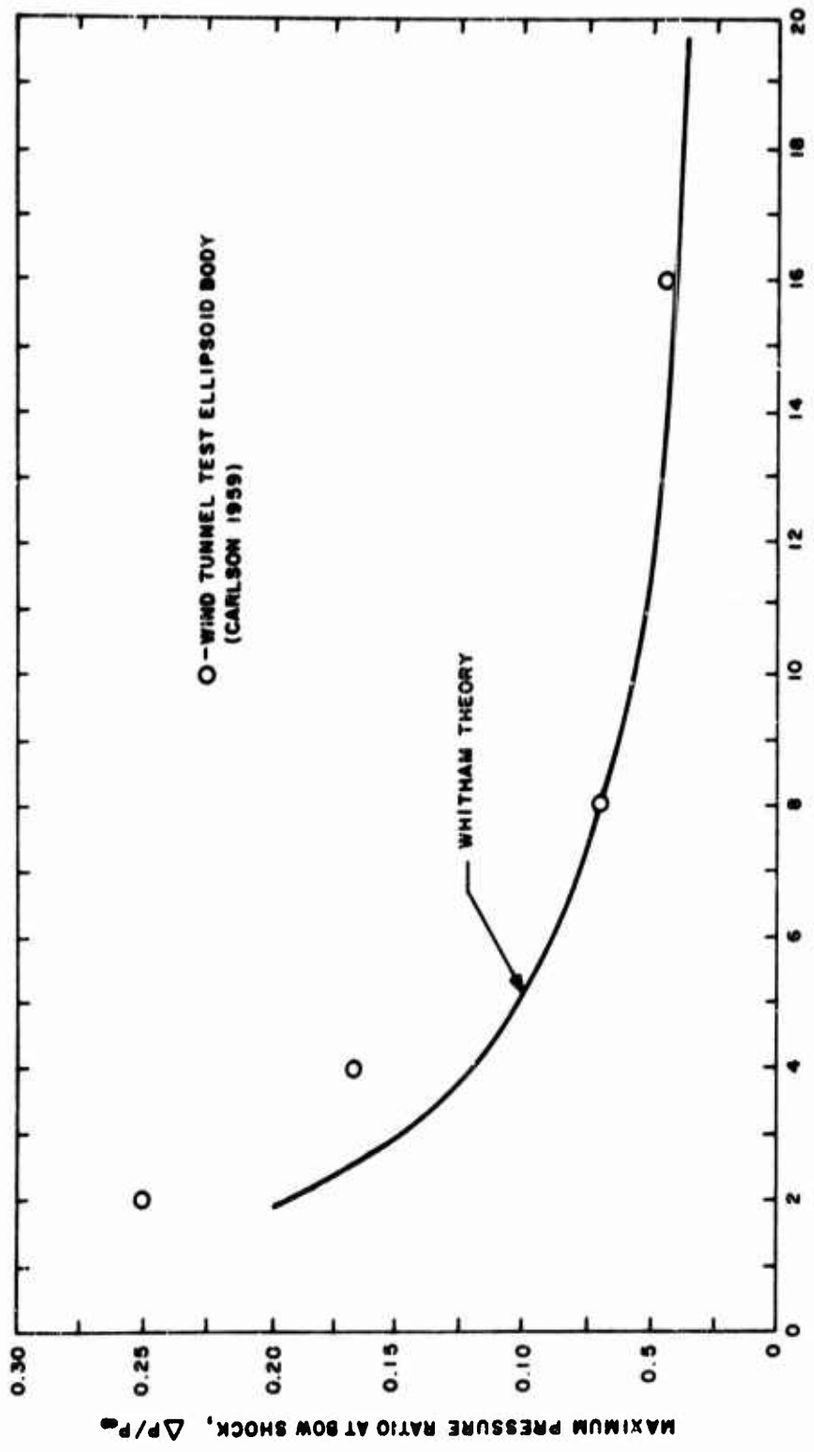

Figure 21. Comparison of Whitham theory with experiment.

Unclassified

Security Classification

DOCUMENT CONTROL DATA - R&D

(Security classification of title, body of abstract and indexing annotation must be entered when the overall report is classified)

1. ORIGINATING ACTIVITY (Corporate author) MITHRAS, Inc. 701 Concord Avenue Cambridge, Massachusetts 02138	2a. REPORT SECURITY CLASSIFICATION Unclassified 2b. GROUP

3. REPORT TITLE

High Altitude Rocket Plumes

4. DESCRIPTIVE NOTES (Type of report and inclusive dates)

Final Scientific Report (Period covering 1 July 1965 - 3 May 1966

5. AUTHOR(S) (Last name, first name, initial)

Jarvinen, P.O., Hill, J.A.F., Draper, J.S., Good, R.E.

6. REPORT DATE	7a. TOTAL NO. OF PAGES	7b. NO. OF REFS
June 1966	vi and 66	11

8a. CONTRACT OR GRANT NO.	9a. ORIGINATOR'S REPORT NUMBER(S)
AF19(628)-4218 b. PROJECT NO. 4691-07 c. 62405454 d. 674691	MC 65-120-R3 9b. OTHER REPORT NO(S) (Any other numbers that may be assigned this report) AFCRL-66-656

10. AVAILABILITY/LIMITATION NOTICES

This document is subject to special export controls and each transmittal to foreign governments or foreign nationals may be made only with prior approval of Air Force Cambridge Research Laboratories.

11. SUPPLEMENTARY NOTES	12. SPONSORING MILITARY ACTIVITY
	Hq., AFCRL, OAR (CRU) United States Air Force L G Hanscom Field, Bedford, Massachusetts

13. ABSTRACT

The gasdynamic structure of high altitude rocket plumes is investigated. A simple analytical model for the expansion of a gas into a vacuum is constructed and is shown to represent the expansion of exhaust gases from rocket motors into the region bounded by the inner shock wave and Mach disc. A comparison of the exhaust expansion model with solutions obtained with the method of characteristics is made and shows good agreement. Contours of constant density, electron density, and collision frequency in the exhaust plume of a typical rocket engine are determined.

The blast wave theory of Hill et al is extended to allow the calculation of the size and shape of rocket plumes of solid propellant missiles. A method is derived which determines the plume drag of solid propellant motors. The method accounts for the fact that solid propellant rocket plume flow is a two phase flow of gas and solids and that the solids present in the exhaust take part in determining the mass flow but not the pressure or the expansion of the exhaust gases upon exit from the rocket nozzle. The plume expansion and resulting plume size is shown to depend on the thrust and the engine exit plane conditions of the gas phase of the two phase flow.

In the addendum to this report, a high altitude plume ionization model is developed using the theoretical models for exhaust flow, two phase rocket motor flow and properties of the air-exhaust gas layer.

DD FORM 1 JAN 64 1473

Unclassified

Security Classification

Unclassified

Security Classification

14 KEY WORDS	LINK A		LINK B		LINK C	
	ROLE	WT	ROLE	WT	ROLE	WT
Rocket Plumes						
Exhaust Plumes						
Supersonic Jet Flow						
Solid Propellant Exhaust Plumes						
Two Phase Nozzle Flow						
Plume Characteristics						
Jets						

INSTRUCTIONS

1. **ORIGINATING ACTIVITY:** Enter the name and address of the contractor, subcontractor, grantee, Department of Defense activity or other organization *(corporate author)* issuing the report.

2a. **REPORT SECURITY CLASSIFICATION:** Enter the overall security classification of the report. Indicate whether "Restricted Data" is included. Marking is to be in accordance with appropriate security regulations.

2b. **GROUP:** Automatic downgrading is specified in DoD Directive 5200.10 and Armed Forces Industrial Manual. Enter the group number. Also, when applicable, show that optional markings have been used for Group 3 and Group 4 as authorized.

3. **REPORT TITLE:** Enter the complete report title in all capital letters. Titles in all cases should be unclassified. If a meaningful title cannot be selected without classification, show title classification in all capitals in parenthesis immediately following the title.

4. **DESCRIPTIVE NOTES:** If appropriate, enter the type of report, e.g., interim, progress, summary, annual, or final. Give the inclusive dates when a specific reporting period is covered.

5. **AUTHOR(S):** Enter the name(s) of author(s) as shown on or in the report. Enter last name, first name, middle initial. If military, show rank and branch of service. The name of the principal author is an absolute minimum requirement.

6. **REPORT DATE:** Enter the date of the report as day, month, year; or month, year. If more than one date appears on the report, use date of publication.

7a. **TOTAL NUMBER OF PAGES:** The total page count should follow normal pagination procedures, i.e., enter the number of pages containing information.

7b. **NUMBER OF REFERENCES:** Enter the total number of references cited in the report.

8a. **CONTRACT OR GRANT NUMBER:** If appropriate, enter the applicable number of the contract or grant under which the report was written.

8b, 8c, & 8d. **PROJECT NUMBER:** Enter the appropriate military department identification, such as project number, subproject number, system numbers, task number, etc.

9a. **ORIGINATOR'S REPORT NUMBER(S):** Enter the official report number by which the document will be identified and controlled by the originating activity. This number must be unique to this report.

9b. **OTHER REPORT NUMBER(S):** If the report has been assigned any other report numbers *(either by the originator or by the sponsor)*, also enter this number(s).

10. **AVAILABILITY/LIMITATION NOTICES:** Enter any limitations on further dissemination of the report, other than those imposed by security classification, using standard statements such as:

(1) "Qualified requesters may obtain copies of this report from DDC."

(2) "Foreign announcement and dissemination of this report by DDC is not authorized."

(3) "U. S. Government agencies may obtain copies of this report directly from DDC. Other qualified DDC users shall request through

_____."

(4) "U. S. military agencies may obtain copies of this report directly from DDC. Other qualified users shall request through

_____."

(5) "All distribution of this report is controlled. Qualified DDC users shall request through

_____."

If the report has been furnished to the Office of Technical Services, Department of Commerce, for sale to the public, indicate this fact and enter the price, if known.

11. **SUPPLEMENTARY NOTES:** Use for additional explanatory notes.

12. **SPONSORING MILITARY ACTIVITY:** Enter the name of the departmental project office or laboratory sponsoring *(paying for)* the research and development. Include address.

13. **ABSTRACT:** Enter an abstract giving a brief and factual summary of the document indicative of the report, even though it may also appear elsewhere in the body of the technical report. If additional space is required, a continuation sheet shall be attached.

It is highly desirable that the abstract of classified reports be unclassified. Each paragraph of the abstract shall end with an indication of the military security classification of the information in the paragraph, represented as *(TS), (S), (C), or (U)*.

There is no limitation on the length of the abstract. However, the suggested length is from 150 to 225 words.

14. **KEY WORDS:** Key words are technically meaningful terms or short phrases that characterize a report and may be used as index entries for cataloging the report. Key words must be selected so that no security classification is required. Identifiers, such as equipment model designation, trade name, military project code name, geographic location, may be used as key words but will be followed by an indication of technical context. The assignment of links, rules, and weights is optional.

GPO 886-551

Unclassified

Security Classification